Two Functionally Different Na/K Pumps in Cardiac Ventricular Myocytes

J. GAO, R. T. MATHIAS,* I. S. COHEN, and G. J. BALDO

From the Department of Physiology and Biophysics, State University of New York at Stony Brook, Stony Brook, New York 11794-8661

ABSTRACT The whole-cell patch-clamp technique was used to voltage clamp acutely isolated myocytes at −60 mV and study effects of ionic environment on Na/K pump activity. In quiescent guinea pig myocytes, normal intracellular Na^+ is ~6 mM, which gives a total pump current of 0.25 ± 0.09 pA/pF, and an inward background sodium current of 0.75 ± 0.26 pA/pF. The average capacitance of a cell is 189 ± 61 pF. Our main conclusion is the total Na/K pump current comprises currents from two different types of pumps, whose functional responses to the extracellular environment are different. Pump current was reversibly blocked with two affinities by extracellular dihydro-ouabain (DHO). We determined dissociation constants of 72 μM for low affinity (type-l) pumps and 0.75 μM for high affinity (type-h) pumps. These dissociation constants did not detectably change with two intracellular Na^+ concentrations, one saturating and one near half-saturating, and with two extracellular K^+ concentrations of 4.6 and 1.0 mM. Ion effects on type-h pumps were therefore measured using 5 μM DHO and on total pump current using 1 mM DHO. Extracellular K^+ half-maximally activated the type-h pumps at 0.4 mM and the type-l at 3.7 mM. Extracellular H^+ blocked the type-l pumps with half-maximal blockade at a pH of 7.71 whereas the type-h pumps were insensitive to extracellular pH. Both types of pumps responded similarly to changes in intracellular-Na^+, with 9.6 mM causing half-maximal activation. Neither changes in intracellular pH between 6.0 and 7.2, nor concentrations of intracellular K^+ of 140 mM or below, had any effect on either type of pump. The lack of any effect of intracellular K^+ suggests the dissociation constants are in the molar range so this step in the pump cycle is not rate limiting under normal physiological conditions. Changes in intracellular-Na^+ did not affect the half-maximal activation by extracellular K^+, and vice versa. We found DHO-blockade of Na/K pump current in canine ventricular myocytes also occurred with two affinities, which are very similar to those from guinea pig myocytes or rat ventricular myocytes. In contrast, isolated canine Purkinje myocytes have predominantly the type-h pumps, insofar as DHO-blockade and extracellular K^+ activation are much closer to our type-h results than type-l. These observations suggest for mammalian ventricular myocytes: (*a*) the presence of two types of Na/K pumps may be a general property. (*b*) Normal physiological variations in extracellular pH and K^+ are im-

Address correspondence to Richard T. Mathias, Department of Physiology and Biophysics, SUNY, Stony Brook, Health Sciences Center, BHS Tower T-6, Stony Brook, NY 11794-8661.

J. GEN. PHYSIOL. © The Rockefeller University Press · 0022-1295/95/10/995/36 $2.00
Volume 106 November 1995 995–1030

portant determinants of Na/K pump current. (*c*) Normal physiological variations in the intracellular environment affect Na/K pump current primarily via the Na^+ concentration. Lastly, Na/K pump current appears to be specifically tailored for a tissue by expression of a mix of functionally different types of pumps.

INTRODUCTION

The Na/K pump is an ubiquitous enzyme that establishes cellular transmembrane Na^+ and K^+ gradients. These gradients are essential for cell volume regulation, are widely used to generate electrical activity, and the Na^+ gradient drives a host of secondary active transport processes. During each cycle, one ATP is cleaved, two K^+'s are transported into the cell and three Na^+'s are transported out of the cell. Thus, the pump cycle results in net outward movement of positive charge and is electrogenic, contributing a current that hyperpolarizes the membrane (Rang and Ritchie, 1968; Gadsby and Cranefield, 1979).

In some tissues, like heart, the current generated by the pump has important direct effects on electrical activity (Gadsby and Cranefield, 1982). For example, in the guinea pig ventricular cells used for this study, we estimate the net outward current during the plateau phase of the action potential to be 0.08–0.09 $\mu A/\mu F$ whereas Na/K pumps generate on the order of 0.5 $\mu A/\mu F$ at these plateau voltages (Gadsby and Nakao, 1989). Thus, even a small transient change in pump current dramatically alters action potential duration. Previous work has shown Na^+, K^+, and voltage (Gadsby and Nakao, 1989; Nakao and Gadsby, 1989), as well as autonomic input (Gao, Mathias, Cohen, and Baldo, 1992) will indeed transiently alter the pump current in these cells. Moreover, the action potential differs in different regions of the heart. Hence, one suspects the pump current may be tailored to generate a specific regional action potential, just like the ion channels are tailored. One mechanism of doing so is to express different ratios of the Na/K pump types in different tissues.

In vivo, the pump comprises an α and β subunit though in vitro studies have shown the α subunit alone binds Na^+ and K^+, splits ATP and has its ATPase activity blocked by the cardiac glycosides (Sweadner, 1985). Sweadner (1989) and Geering (1990) review recent data demonstrating the Na/K pump is a multigene family of proteins. To date, three isoforms of the α subunit and two of the β have been identified. The distribution of β isoforms has not been widely studied; however, the α isoforms are expressed in a tissue-specific manner, and in heart, the $\alpha 1$ and $\alpha 2$ (or sometimes $\alpha 3$) isoforms have been found in ventricular muscle (Berrebi-Bertrand, Maixent, Guede, Gerbi, Charlemagne, and Lelievre, 1991; Sweadner, Herrera, Amato, Moellmann, Gibbons, and Repke, 1994) whereas the $\alpha 2$ and $\alpha 3$ predominate in Purkinje fibers (Zahler, Brines, Kashgarian, Benz, and Gilmore-Herbert, 1992; Zahler, Gilmore-Herbert, Baldwin, Franco, and Benz, 1993). These observations also suggest specific functions for the pumps in each tissue. However, various Na^+ and K^+ environments have shown little difference in the $\alpha 1$, $\alpha 2$, and $\alpha 3$ isoform ATPase activity in vitro (Sweadner, 1985; Brodsky and Guidotti, 1990; Guillaume, Grisar, Delgado-Escueta, Laschet, and Bureau-Hereen, 1990; Jewell and Lingrel, 1991), though the glycoside sensitivity of $\alpha 1$ is ~100-fold lower than that of $\alpha 2$ or

α3 (Sweadner, 1985; Gupta, Chopra, and Stetsko, 1986; Orlowski and Lingrel, 1988). Nevertheless, the functional properties of these isoforms in an intact cell are not well known. Mogul, Rasmussen, Singer, and Ten Eick (1989) first showed DHO-blockade of pump current in guinea pig ventricular myocytes occurs with two different affinities. We verified their result, which suggested two types of Na/K pumps coexist in these cells, possibly corresponding to two α isoforms. We repeated the DHO-blockade study in canine ventricular myocytes and again found two affinities. Berlin, Fielding, and Ishizuka (1992) performed sinilar studies in rat ventricular myoctes with similar results. Given the observations above, we began experiments to test for functional differences between these two types of pump in guinea pig. The purpose of this paper is to describe the effects of various ionic environments on transport by each pump type.

GLOSSARY

Subscripts

ATP	adenosine tri-phosphate
D	dihydro-ouabain
h	high affinity type pumps
H	hydrogen
i	intracellular
ib	inward background sodium flux
in	input resistance or capacitance of the cell
K	potassium
l	low affinity type pumps
max	maximum Na/K pump current
Na	sodium
Na/K	sodium/potassium pumps
o	extracellular
p	pipette
t	transverse tubular system
T	total pumps, both high and low affinity

Symbols

C	(F)	capacitance
D	(cm^2/s)	diffusion coefficient $\simeq 1.5 \times 10^{-5}$ cm^2/s for sodium
l[DHO]	(M)	concentration of dihydro-ouabain
$E_{1,2}$		the two major configurations of the Na/K pumps, 1 implies intracellular cations interact with the pump, and 2 implies extracellular cations interact
E	(V)	equilibrium potential
$f_{h,l}$		fractions of type-h or type-l pump current under specific conditions
$F_{h,l}$		fraction of type-h or type-l pump molecules
F		(coul/mole) Faraday constant $\simeq 10^5$ coul/mole
i	($A/\mu F$)	current density if membrane capacitance is 1 $\mu F/cm^2$
I	(A)	current
j	(mole/s)	flux

K	(M)	dissociation constant
[K]	(M)	potassium concentration
l	(cm)	characteristic length
P		probability of binding
Q		probability of not binding
R	(Ω)	resistance
RT/F	(V)	constant ≈26 mV
S	(cm^2)	surface area
V	(cm^3)	volume
ψ	(V)	voltage
ρ	(Ω-cm)	resistivity of pipette solution ≈60 Ω-cm
τ	(s)	time constant
ω	(cm/s)	permeability
ζ		tortuosity factor for the t-system

METHODS

Cardiac ventricular myocytes were isolated from adult male Hartley guinea pigs, as described in Gao, Mathias, Cohen, and Baldo (1992) and initially worked out by Isenberg and Klockner (1982) or from mongrel dogs as described in Cohen, Datyner, Gintant, Mulrine, and Pennefather (1987) and Yu, Chang, and Cohen (1993). The isolated cells were studied using the whole-cell patch-clamp technique (Marty and Neher, 1983). Patch pipettes of initial resistance 1–2 MΩ were pulled from KG-12 glass (Garner Glass Co., Claremont, CA) using a two-step procedure on a Kopf microelectrode puller (model 750, David Kopf Instruments, Tujunga, CA). The studies were conducted using an Axopatch 1A amplifier (Axon Instruments, Burlingame, CA). Seal resistances were 10–20 GΩ. After achieving a seal and rupturing the underlying cell membrane, we waited at least 5 min for the pipette and cell solutions to come to steady state. The pipette resistance, R_p, was estimated from the initial ($t = 0$) jump in voltage after a step in current with values ranging from 3 to 6 MΩ. We then voltage clamped the cells to −60 mV and measured Na/K pump current as the decrease in outward current produced by extracellular application of the cardiac glycoside dihydro-ouabain (DHO), a specific reversible inhibitor of Na/K pump activity in these cells (Gao et al., 1992). We use 1 mM DHO to block roughly 96% of the total pump current and 5 μM DHO to block current that is typically 89% from the high affinity type pumps. These percentages vary somewhat depending on the conditions of the experiment, but to the resolution of our data, we equate ion effects on I_T with the 1 mM DHO blockade and ion effects on I_h with the 5 μM DHO blockade. The properties of the low DHO affinity current are then proportional to the difference, $I_l = I_T - I_h$. In most experiments we use a current clamp step to determine the cell's input capacitance and resistance and the pipette's tip resistance. The input capacitance is used as a measure of cell membrane area to normalize the currents (e.g., $i_T = I_T/C_{in}$, $i_T = i_h + i_l$).

Solutions

Our standard pipette solution contained (in millimolar): 5 Na_2-ATP, 40 NaCl, and KCl 2 for the $[Na]_p$ = 50 mM studies or NaCl 0 and KCl 42 for the $[Na]_p$ = 10 mM studies; K-Aspartic acid 40; KH_2PO_4 10; $MgSO_4$ 1; HEPES 5; EGTA 11; $CaCl_2$ 1; glucose 10. In generating the $[Na]_i$-activation curve, we substituted Na^+ for K^+. The external solution contained (in millimolar): 137.7 NaCl; 2.3 NaOH; 1 $MgCl_2$; 10 glucose; 5 HEPES; 4.6 KCl; 1.8 $CaCl_2$; 0.5 $BaCl_2$; 0.2 $CdCl_2$. When $[K]_o$ was altered, we substituted Na^+ for K^+. DHO was simply added to the above external solution. Solution pH was adjusted by titration with HCl or NaOH to obtain pH_o = 7.4 and pH_i = 7.2 in normal conditions, or as indicated in pH studies.

Experimental Limitations

Changes in membrane currents during these experiments are rather slow so the small input capacitance of the cell poses no problem to our voltage clamp. However, the tip resistance of the pipette R_p in series with the cell's input resistance R_{in} makes a resistor divider network for the measurement of pump current. It can be shown that the measured current is reduced by $R_{in}/(R_p + R_{in})$. The highest resistance pipette after going to the whole-cell patch mode was 6 MΩ, so a worst-case error in normal Tyrode solution (R_{in} = 19 MΩ) is 24%. To avoid such large errors or the need for correction, we added Ba^{2+} to the Tyrode in all of the experiments reported here. This blocked the background K^+ conductance and increased R_{in} to ~200 MΩ, making the worst-case error ~3%, which we neglect.

We sometimes measured small changes in current in the presence of significant background noise. To do this, a relatively rapid bath exchange (13-s time constant) with a constant temperature (36°C) is essential to distinguish the characteristic time course of DHO blockade from random drift. Nevertheless, baseline drift limits our resolution to ~10 pA. Whenever possible, changes in pump function are measured relative to a control in the same cell, thus removing cell to cell variability. In experiments which successfully measure control-test-recontrol currents, total pump current shows no indication of run down (a ratio of recontrol-to-control of 1.0 ± 0.03, mean ± SD for n = 13 with times ranging from 20–40 m).

The major limitation of the whole-cell patch-clamp technique in these experiments is control of intracellular sodium, $[Na]_i$. As described in Mathias, Cohen, and Oliva (1990) the small tip of the patch pipette is a significant barrier to diffusion, hence, when a net transmembrane Na^+ flux is generated, a concentration difference develops between pipette sodium, $[Na]_p$, and cell. That is, if we perturb the total pump current I_T (A), given an inward background Na^+-current I_{ib} (A), the net transmembrane Na^+ flux out of the cell is $(3I_T - I_{ib})/F$(mol/s). At steady state the Na^+ flux from the pipette into the cell must equal the transmembrane flux. Mathias et al. (1990) show the Na^+ flux between pipette and cell has the following dependence on $[Na]_i$ and $[Na]_p$:

$$\frac{\rho D_{Na}}{R_p}([Na]_p - [Na]_i) = (3I_T - I_{ib})/F \tag{1}$$

where $\rho(\Omega-cm)$ is the resistivity of the pipette solution, R_p (Ω) is the resistance of the pipette tip, and the ratio ρ/R_p(cm) describes the effect of an arbitrary tip geometry on the diffusion of Na^+. D_{Na} (cm^2/s) is the diffusion coefficient for Na^+. Using the whole-cell patch-clamp technique, we can experimentally measure R_p, I_T,and I_{ib}, leaving $[Na]_i$ as the only variable not measured, but Eq. 1 can be solved to obtain $[Na]_i$ in steady state experimental conditions. This technique is used to obtain our best estimate of the dependence of pump currents on $[Na]_i$.

For studies in which extracellular ions are changed, our test measurement of pump current was made as soon as possible after the change in bath composition, thus minimizing the time for changes in $[Na]_i$. Nevertheless, some changes still occur. If the experiment begins in the steady state condition given by Eq. 1 with $[Na]_i(0)$ corresponding to $I_T(0)$, the change in $[Na]_i$ can be determined from the change in pump current. Viz, define

$$\begin{aligned} \Delta[Na]_i(t) &= [Na]_i(t) - [Na]_i(0) \\ \Delta I_T(t) &= I_T(t) - I_T(0) \end{aligned} \tag{2}$$

then

$$V_i \frac{d\Delta[Na]_i(t)}{dt} = -\frac{\rho D_{Na}}{R_p}\Delta[Na]_i(t) - \frac{3\Delta I_T(t)}{F}, \tag{3}$$

which has the solution

$$\Delta [Na]_i(t) = \frac{1}{V_i F}\int_0^t \exp\{(t-s)/\tau_p\}\,\Delta I_T(s)ds \quad (4)$$

where V_i (cm^3) is the cell volume and

$$\tau_p = \frac{V_i R_p}{\rho D_{Na}}. \quad (5)$$

We can experimentally measure V_i, R_p and $\Delta I_T(t)$ so the integral in Eq. 4 can be evaluated to obtain $\Delta[Na]_i(t)$. Our experimentally measured I_T vs $[Na]_i$ curve determines how our test conditions would have affected pump current had there been no change in $[Na]_i$. That is, we separate the direct effect of the test condition from its indirect consequence due to a change in $[Na]_i$.

One other potential source of artifact is changes in extracellular K^+ in the t-system lumen. However, as analyzed in the Appendix, the structural and electrical properties of the myocytes suggest these changes are negligible.

RESULTS

The passive electrical properties of isolated ventricular myocytes from guinea pig hearts are described in the Appendix. We measure Na/K pump function by whole-cell patch clamping at $\psi_i = -60$ mV and recording the change in current produced by the cardiac glycoside dihydro-ouabain (DHO). Gao et al. (1992) have shown DHO has no effect on membrane conductance in these cells. However, as described above, uncontrolled changes in $[Na]_i$ can cause significant artifacts in the measurement of Na/K pump function. In the following results, we first present data used to estimate the inward background Na^+ current, which is subsequently used to estimate artifactual changes in $[Na]_i$ after alteration of the Na/K pump current. We then assess the effects of $[Na]_i$, $[K]_i$, $[K]_o$, pH_o, and pH_i on transport by each type pump.

Inward Background Na^+ Current

We estimate I_{ib} in two ways. The upper panel in Fig. 1 illustrates a direct electrical measurement. In this experiment, the extracellular solution is normal Tyrode and the intracellular solution is adjusted so that $E_K = E_{Cl} = -90$ mV and $[Na]_i = 6$ mM. We block I_T with 1 mM DHO then step ψ_i to -90 mV, where K^+ and Cl^- are in equilibrium. Under these conditions, the only significant remaining current is I_{ib}. However, this procedure gives the value of I_{ib} at $\psi_i = -90$ mV whereas our experiments are conducted at $\psi_i = -60$ mV. To correct for the voltage change, we assume I_{ib} is described by the constant field equation with a voltage-independent permeability coefficient, ω_{Na} (Eisner and Smith, 1981). The current density is then

$$i_{ib} = \omega_{Na}\frac{F^2\psi_i}{RT}\frac{[Na]_i e^{F\psi_i/RT} - [Na]_0}{e^{F\psi_i/RT} - 1}\ (A/cm^2). \quad (6)$$

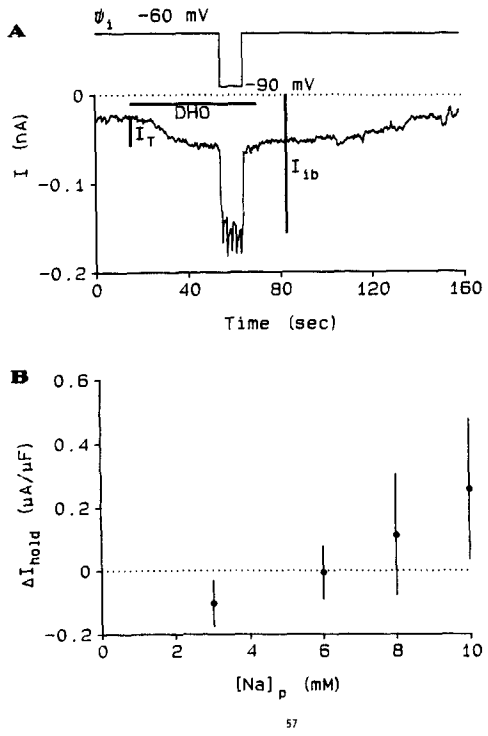

FIGURE 1. Measurement of the inward background sodium current, I_{ib} (*A*) In the upper panel, we set the concentrations of K^+ and Cl^- so the Nernst potentials $E_K = E_{Cl} = -90$ mV, apply a saturating dose of DHO to block the total pump current I_T, then voltage clamp the intracellular voltage $\psi_i = -90$ mV and record the inward background current. Since potasssium and chloride are at equilibrium and Na/K pumping is blocked, the majority of I_{ib} should be carried by sodium. The value of I_{ib} thus measured is adjusted to describe our experiments at $\psi_i = -60$ mV (see Eq. 6) and normalized to the input capacitance as a measure of membrane area (see Eq. 7). The graph in the bottom panel illustrates how we estimate the normal resting value of $[Na]_i = 6$ mM at $\psi_i = -60$ mV in the dissociated cells. The change in holding current is measured from the time just after breaking the membrane between the pipette and cell until diffusion of $[Na]_p$ into the cell reaches steady state (~5 m). If $[Na]_p$ is greater than normal $[Na]_i$, the Na/K pumps are stimulated and the change in holding current is outward, whereas if $[Na]_p$ is less than normal $[Na]_i$ the pumps are inhibited and the change in holding current is inward. We use this result to determine I_{ib} by setting $[Na]_i = 6$ mM with normal Tyrode outside and applying a saturating concentration of DHO to block total Na/K pump activity. Since $[Na]_i$ is at its normal steady state value, $3\ I_T = I_{ib}$, assuming 3 Na^+ are extruded per cycle. The value thus obtained is given in Eq. 8.

Using Eq. 6, the value of I_{ib} in Fig. 1 should be reduced by 28% to correct for the voltage shift of 30 mV. From five cells we determined that, at $\psi_i = -60$ mV,

$$i_{ib} = 0.75 \pm 0.21 \ \mu A/\mu F \tag{7}$$

and $\omega_{Na} = 2 \times 10^{-8}$ cm/s, assuming a membrane capacitance of 1 $\mu F/cm^2$.

The second method of determining I_{ib} used the measured pump current. At normal steady state conditions, $I_{ib} = 3I_T$ for a 3 Na^+:2 K^+ stoichiometry. However, I_T is sensitive to $[Na]_i$ so we need to know normal $[Na]_i$ in unpatched quiescent isolated cells. We estimated normal $[Na]_i$ from the results shown in the lower panel of Fig. 1. After rupturing the patch of membrane in the pipette tip, the holding current drifted with a time constant predicted for diffusion of the pipette solution into the cells; the direction of the drift depended on the pipette sodium concentration $[Na]_p$. Our interpretation is that when $[Na]_p$ is higher than normal intracellular sodium, the pump is stimulated and the holding current becomes more outward. Vice versa when $[Na]_p$ is below normal $[Na]_i$. The normal value of $[Na]_i$ is the value

of $[Na]_p$ at which no drift occurs, or 6 mM as seen in the lower panel of Fig. 1. With $[Na]_p$ = 6 mM, the current blocked by 1 mM DHO is 0.24 ± 0.08 μA/μF from eight cells. Because 1 mM DHO blocks 96% of the total pump current in these conditions, the normal pump current is 0.25 ± 0.09 μA/μF and the Na^+-current is three times this value:

$$i_{ib} = 0.75 \pm 0.26\ \mu A/\mu F. \tag{8}$$

These two methods did not have to be in such good agreement, since there could be a significant but electrically silent Na^+ influx (e.g., Na^+/H^+ exchange, et cetera) or i_{ib} could include significant current carried by ions other than Na^+. The electrical method of Eq. 7 would not include neutral exchange fluxes but would include non-Na^+ fluxes. We therefore conclude the majority of the background current is carried by Na^+ and the majority of Na^+ influx is not electrically silent, at least under these conditions.

Na/K Pump Currents

The data that follow suggest the presence of two types of pumps. This interpretation leads to some surprising predictions on the properties of the overall current, i_T. Assume the total pump current is the sum of the type-h and type-l pump currents.

$$i_T = i_h + i_l. \tag{9}$$

Our data suggest pH_o affects i_l but not i_h and $[K]_o$-activation of i_l is very different from that of i_h. Eq. 9 predicts the DHO-blockade curve for i_T depends on pH_o and $[K]_o$, the $[K]_o$-activation curve for i_T depends on pH_o and the $[H]_o$-blockade curve for i_T depends on $[K]_o$. To discuss our results in the context of two pumps, it is useful to write down the model. We therefore preview here our conclusions.

If pump current is normalized by its maximum value, the probability of activating the current by $[K]_o$ appears to be independent of $[Na]_i$, and vice versa. This means ion activation data for either type pump are described by $i = i_{max} P_{Na} P_K$, where P_{Na} and P_K are Michaelis-Menten type functions that go from 0 to 1 as concentration goes from 0 to ∞. An analytic expression for P_{Na} or P_K is not well determined by the data, as a variety of models provide an adequate fit.

Before combining the ideas of independence and two pumps, we can somewhat simplify the resulting expression by including our observation P_{Na} is essentially the same for both types of pumps. Conversely, P_K is very different for the two pumps so P_{Kh} and P_{Kl} are subscripted to indicate which is being considered. The result is

$$i_T = i_{maxh} P_{Na} P_{Kh} + i_{maxl} P_{Na} P_{Kl}. \tag{10}$$

Lastly, our data show i_{maxl} is reduced by an increase in $[H]_o$ whereas i_{maxh} is not. The reduction of i_{maxl} by $[H]_o$, over the range of concentrations we could study, is adequately described by one pump blocked for one H^+ bound. The value of i_{maxl} is thus dependent on Q_H, which is the fraction of type-l pumps without an H^+ bound.

$$Q_H = \frac{K_H}{[H]_0 + K_H} \tag{11}$$

For convenience, we assume the two types of pumps have the same maximum turnover rate, hence maximum current depends on the fraction of a particular type pump. Let F_h be the fraction of type-h pumps in these cells, then combining our various observations with this assumption yields

$$\begin{aligned} i_T &= i_{max} P_{Na}[F_h P_{Kh} + (1 - F_h) P_{Kl} Q_H] \\ i_h &= i_{max} P_{Na} F_h P_{Kh} \\ i_l &= i_{max} P_{Na}(1 - F_h) P_{Kl} Q_H. \end{aligned} \tag{12}$$

In the following results, we do not use Eq. 12 to fit the data, rather, it is a conclusion which is consistent with all of the data.

DHO Blockade of Pump Current

Fig. 2 and Table I illustrate the blockade of ventricular Na/K pump current by the cardiac glycoside DHO. Fig. 2 *A* shows a typical protocol for obtaining the data. We compare the current blocked by a test concentration of DHO (in this case 0.01 mM) with the current blocked by 1 mM, which is the control concentration applied to each myocyte; the order of application was random. As a result of the protocol, data in Table I are normalized such that blockade by 1 mM DHO is unity with no standard deviation and other concentrations cause relative fractional blockade ± standard deviations. Mean values and standard deviations for pump current blocked by 1 mM DHO are listed in Table II for various concentrations of pipette sodium. The curves in Fig. 2 (*B–D*) are mean values from Table I scaled by the theoretically projected maximum total current blocked at infinite [DHO]; the current blocked by 1 mM DHO is ~96% of the projected maximum.

The data in Fig. 2 were fit with the two-site model:

$$P_{DT} = \frac{i_h}{i_T} \frac{[DHO]}{[DHO] + K_{Dh}} + \frac{i_l}{i_T} \frac{[DHO]}{[DHO] + K_{Dl}}. \tag{13}$$

There appears to be no significant difference in DHO blockade at $[Na]_p$ = 10 vs 50 mM so these data were grouped together in Fig. 2 *B* and fit with Eq. 13. The best fit parameters are given in Eq. 14. The weighted high- and low-affinity binding curves from Eq. 13 are graphed as dashed lines in Fig. 2 *B* whereas the weighted sum (P_{DT}) is the solid line. These data illustrate effects of DHO from 200 nM to 1 mM, a range incompatible with a single binding site. Moreover the shape of the blockade curve suggests the presence of two different binding sites, whose dissociation constants are well separated, regardless of $[Na]_i$. The vertical dashed line in Fig. 2 *B* marks the 5-μM DHO point and suggests ~89% of the current blocked by 5 μM DHO comes from type-h pumps. Moreover, the ratio of i_h/i_T is well approximated by the entry under 5 μM DHO in Table I. The average fraction of 0.37 as measured in the same cell compares well with the Table II average fraction of 0.33 which was measured in different populations of cells and at various values of $[Na]_p$. Tables I and II and Fig. 2 each suggest $[Na]_i$ has no significant effect on DHO binding in these cells.

There are many studies showing an interaction between $[K]_o$ and glycoside binding/blockade (reviewed in Eisner and Smith, 1991). Apell and Sturmer (1992) re-

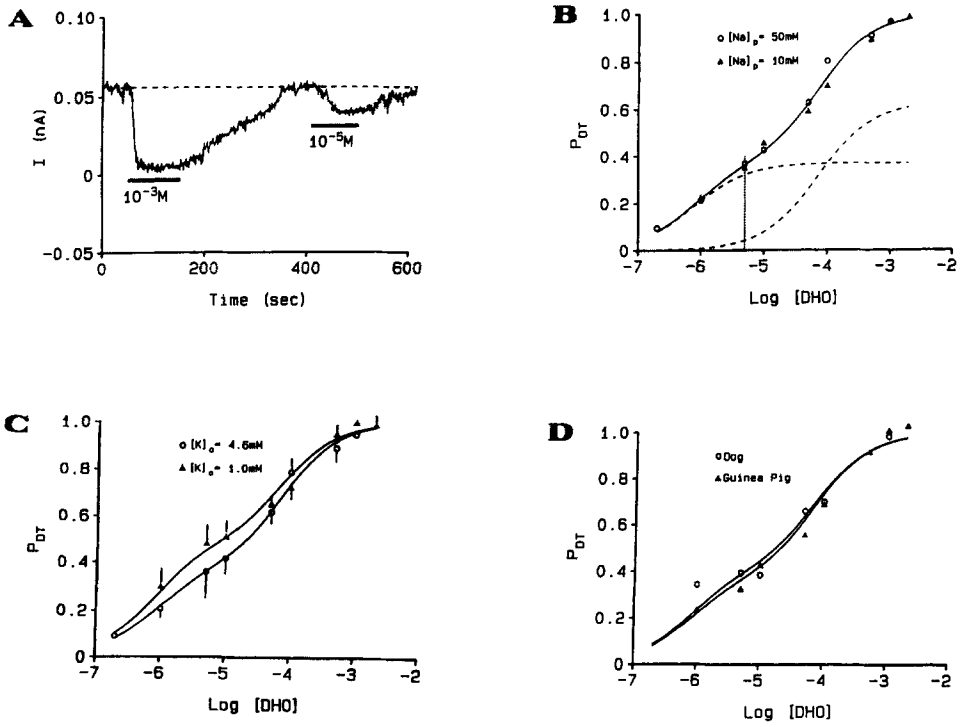

FIGURE 2. DHO blockade of ventricular Na/K pumps. (*A*) A typical protocol for measuring DHO blockade as the fraction of total Na/K pump current blocked by a given concentration. In the same cell, the current blocked by [DHO] = 1 mM (*control*) and by a test [DHO] is recorded. The ratio of test to control gives the relative blockade, which may or may not give relative binding depending on $[Na]_i$. (*B*) A comparison of DHO blockade at different values of $[Na]_i$ with $[K]_o$ = 4.6 mM. To the resolution of our data, $[Na]_i$ appears to have no effect on DHO binding. The individual binding curves for low- and high-affinity pumps are shown as dashed curves. The vertical dashed line indicates 5 μM [DHO], which we use to measure i_h. (*C*) The effect of $[K]_o$ on DHO blockade with 50 mM $[Na]_p$. The two curves have the same dissociation constants, but the fraction i_h/i_T = 0.37 in 4.6 mM $[K]_o$ whereas i_h/i_T = 0.48 in 1.0 mM $[K]_o$. Standard deviations are shown to indicate the significance of differences in i_h/i_T for the two curves. Moreover, we tested whether the DHO concentrations of 10^{-5}, 5×10^{-6}, and 10^{-6} M were statistically different at the two values of $[K]_o$ and determined the probability of the differences being due to random variability is <0.01. Because the data are ratios, to perform the statistical analysis the arcsine transformation of the square root of each data point was first employed to stabilize the variance (Sachs, 1982, p269). The analysis was then performed using the GLM procedure from the SAS statistical software package. (*D*) A comparison of DHO-binding in cardiac ventricular cells from guinea pigs and dogs. These data suggest the presence of high and low affinity DHO binding is a property of mammalian ventricular cells rather than a species specific property of guinea pig.

ported DHO binds to those states in which $[Na]_o$ interacts with the pumps. This implies increasing $[K]_o$ reduces DHO binding through a type of kinetic competition by shifting the occupancy away from the Na^+-release states to the K^+-binding states. We looked for these effects of $[K]_o$ on DHO blockade. Fig. 2 *C* compares DHO

TABLE I

DHO Blockade

	Conditions		[DHO]								
	$[Na]_p$	$[K]_o$	2×10^{-3}	10^{-3}	5×10^{-4}	10^{-4}	5×10^{-5}	10^{-5}	5×10^{-6}	10^{-6}	2×10^{-7}
	mM	*mM*	*M*								
Dog raw	10	4.6		1.0		0.68 ± .08	0.63 ± .05	0.33 ± .04	0.36 ± .08	0.31 ± .03	
Corr.	10	4.6		1.0		0.71 ± .08	0.67 ± .05	0.39 ± .05	0.40 ± .09	0.35 ± .03	
G.P. raw	10	4.6	1.02 ± .11	1.0	0.91 ± .14	0.68 ± .08	0.55 ± .09	0.42 ± .16	0.32 ± .08	0.20 ± .03	
Corr.	10	4.6	1.02 ± .11	1.0	0.92 ± .14	0.72 ± .08	0.61 ± .10	0.47 ± .18	0.36 ± .09	0.23 ± .04	
G.P.	50	4.6		1.0	0.94 ± .06	0.83 ±.06	0.65 ± .05	0.44 ± .07	0.38 ± .11	0.22 ± .04	0.09 ± .01
G.P.	50	1.0	0.99 ± .04	1.0	0.95 ± .04	0.72 ± .05	0.65 ± .03	0.51 ± .07	0.48 ± .08	0.30 ± .07	

Entries are mean ± SD for four to seven experiments. In each experiment, the current blocked by 10^{-3} M [DHO] is recorded and compared with blockade at a test [DHO] to obtain the relative fractional blockade. When the test [DHO] is applied, $[Na]_i$ begins to increase and stimulate the pumps that are not blocked. For $[Na]_p$ = 50 mM, the effect is negligible but for $[Na]_p$ = 10 mM a correction was made to estimate the true binding curve. The correction was as follows. We estimated from Eq. 1, $[Na]_i$ = 6.1 mM when $[Na]_\rho$ = 10 mM using average parameters from these cells. The total pump current under these conditions will be denoted $i_T(0)$. A concentration of 1 mM DHO approximately blocks $i_T(0)$. For a test concentration of DHO, we measure the current at t s following application. The current not blocked by the test DHO is $(1-P_{DT})i_T(t)$, thus the current blocked is $i_T(0) - (1-P_{DT})i_T(t)$. Our first estimate of P_{DT} ($\hat{P}_{DT}$) is determined by dividing the blocked current by $i_T(0)$ to obtain $\hat{P} = 1 - (1-P_{DT})\, i_T(t)/i_T(0)$. We assume the only difference in $i_T(t)$ and $i_T(0)$ is due to the change in $[Na]_i$ during the period t, which ranged between 12 and 35 s, thus $i_T(0)/i_T(t) = P_{Na}(0)/P_{Na}(t)$, where $P_{Na}(0)$ refers to P_{Na} evaluated at $[Na]_i(0)$ = 6.1 mM and $P_{Na}(t)$ is evaluated at $[Na]_i(t)$, which ranged between 6.6 and 7.2 mM. We solve for the corrected value of $P_{DT} = 1-(1-\hat{P}_{DT})\, P_{Na}(0_i)/P_{Na}(t)$. The raw and corrected values appear in Table I. This procedure is not strictly rigorous since 1 mM DHO blocks ~96% of i_T rather than 100%, however, the error can be shown to be <0.5%.

blockade at 1 and 4.6 mM $[K]_o$, with $[Na]_p$ = 50 mM. If the only effect of $[K]_o$ is to compete with DHO, then as $[K]_o$ is decreased, the data should simply shift left to lower values of [DHO] whereas the shape of the curve remains the same. Alternatively, if there were no $[K]_o$-[DHO] competition but the two types of pumps have different K^+ activation curves, then the fraction i_h/i_T would change without a shift

TABLE II

Intracellular Sodium Dependence of the Total and High-Affinity Na/K Pump Currents

$[Na]_p$	I_T	i_T	I_h	i_h	i_h/i_T
mM	*pA*	*μA/μF*	*pA*	*μA/μF*	
3	32 ± 10	0.21 ± 0.06			
6	42 ± 18	0.24 ± 0.08			
8	68 ± 22	0.33 ± 0.09			
10	74 ± 23	0.37 ± 0.09	20 ± 3	0.12 ± 0.02	0.32
15			28 ± 3	0.15 ± 0.03	
20	108 ± 29	0.57 ± 0.15	31 ± 5	0.20 ± 0.03	0.35
30	126 ± 17	0.71 ± 0.13	45 ± 9	0.25 ± 0.05	0.35
40	136 ± 31	0.76 ± 0.07			
50			40 ± 9	0.26 ± 0.06	
60	163 ± 34	0.83 ± 0.15			
80	182 ± 40	0.90 ± 0.20	51 ± 11	0.27 ± 0.06	0.30
100	134 ± 9	0.87 ± 0.11	51 ± 7	0.29 ± 0.04	0.33
∞		0.97		0.32	0.33 ± 0.02

Data are mean ± SD with between 5 and 10 cells for each sodium concentration.

in the midpoint of either component of the DHO blockade curve. The two data sets in Fig. 2 *C* do not appear to be simply shifted versions of one another. Moreover, a curve fit based on this premise (i.e., a fit in which i_h/i_T is kept at 0.37 but K_{Dh} and K_{Dl} are varied) obviously miss-fits the 1 mM $[K]_o$ data (fit not shown). For the fit shown, we fixed K_{Dh} and K_{Dl} at the values determined from 4.6 mM $[K]_o$ data, then varied i_h/i_T to generate the theory curve from Eq. 13. This yielded $i_h/i_T = 0.48$ as summarized in Eq. 14. A third possibility is both $[K]_o$-[DHO] competition and differences in the $[K]_o$-activation curves are present. To test this, we varied i_h/i_T, K_{Dh} and K_{Dl}. This reduced the sum-squared error for the fit to the 1 mM $[K]_o$ data, but the theory curve was visually no better a fit than that shown. Moreover, the best fit value of K_{Dl} was shifted to a higher [DHO], which is opposite to competition, whereas the best fit K_{Dh} remains near 0.75 μM and the fraction i_h/i_T at 0.48. We concluded the fraction i_h/i_T must increase as $[K]_o$ is decreased but variance in the data and insensitivity of the theory to the values of K_{Dh} and K_{Dl} preclude firm conclusions on competition. Based on these various fits of the data, we estimate the K_Ds are only known to within about a factor of two. By presenting fits with the same K_Ds for the 4.6 and 1 mM $[K]_o$ data, one can judge whether or not the 1 mM DHO data are competitively shifted to the left of the curve. Irrespective of the absence or presence of competition, an important conclusion from these data is 1 mM DHO blocks i_T whereas 5 μM DHO blocks i_h, regardless of $[K]_o$ in the range we are studying. Moreover, we later show $[K]_o$ activation of i_h occurs at much lower values of $[K]_o$ than does activation of i_l. Thus, dropping $[K]_o$ from 4.6 to 1 mM will reduce i_l, and therefore i_T, but not significantly affect i_h. Under these conditions, the fraction of i_T contributed by i_h should increase, as we have concluded from the analysis of Fig. 2 *C*.

The parameters used to generate the theory curves in Fig. 2, *B* and *C*, are

$$\begin{aligned} K_{Dh} &= 0.75\ \mu M,\ K_{Dl} = 72\ \mu M \\ i_h/i_T &= 0.37 \text{ at } [K]_o = 4.6 \text{ mM} \\ i_h/i_T &= 0.48 \text{ at } [K]_o = 1.0 \text{ mM} \\ i_l/i_T &= 1 - i_h/i_T. \end{aligned} \tag{14}$$

The major effect of $[K]_o$ on the shape of the binding curve arises because i_h/i_T is significantly changed. The DHO blockade data suggest i_h/i_T is independent of $[Na]_i$ but is altered by $[K]_o$ in accordance with Eq. 15, where P_{Kh} and P_{Kl} are later determined from $[K]_o$-activation data and with $pH_o = 7.4$, Q_H is constant.

$$\frac{i_h}{i_T} = \frac{F_h P_{Kh}}{F_h P_{Kh} + (1 - F_h) Q_h P_{Kl}} \tag{15}$$

Although our interpretation assumes no competition between $[K]_o$ and [DHO], half-maximal reduction of i_T does indeed shift to lower values of [DHO] when $[K]_o$ is reduced. For the theory curves in Fig. 2 *C*, half-maximal blockade occurs at [DHO] = 21 μM when $[K]_o$ = 4.6 mM and at [DHO] = 6 μM when $[K]_o$ = 1 mM. The interaction of glycosides, $[K]_o$ and Na/K pumps is obviously complicated in

ventricle and some part of the previously reported competition (reviewed in Eisner and Smith, 1991) is probably due to the presence of two pumps.

Fig. 2 *D* shows the existence of two DHO-binding sites is not a species-specific property of guinea pig ventricle but is also present in dog ventricle. Presumably, the canine ventricular cells also have two functionally different pumps but our subsequent functional studies are limited to guinea pig. In Fig. 2 *D*, we have overplotted the data from dog and guinea pig, with $[Na]_p = 10$ mM for both data sets. The theory curve for the canine data was generated using the values of K_{Dh} and K_{Dl} from guinea pig, with $i_h/i_T = 0.40$. These results suggest the existence of two types of pumps is a general property of cardiac ventricular myocytes. In contrast, Cohen et al. (1987) found the half-saturating concentration of DHO for canine Purkinje cells was 3.7 μM, which is nearer to K_{Dh} than K_{Dl}, suggesting a predominance of type-h pumps in this cell type.

As can be seen from the current records in Fig. 2 *A* the onset of DHO-blockade is much more rapid than removal. For a single binding site and instantaneous addition or removal of [DHO], the time constant for blockade is $(\alpha[\text{DHO}]+\beta)^{-1}$ whereas recovery occurs with the time constant β^{-1}, where

$$[\text{DHO}] + P \underset{\beta}{\overset{\alpha}{\leftrightarrows}} \text{DHO} - P.$$

Our bath exchanges with a time constant of 13 s hence, except for the lowest values of [DHO], the time for onset of blockade is limited by the bath exchange. However, the slower removal of blockade should reflect the properties of the pumps and therefore provide some useful information. Nevertheless, the finite time for the bath exchange significantly affects the time for removal of DHO from its binding sites. Assuming the bath exchange is exponential with time constant τ_b, the equation describing removal of DHO from either type of binding site is

$$\frac{d(\text{DHO} - P)}{dt} = -(\beta + \alpha[\text{DHO}]e^{-t/\tau_b})\,\text{DHO} - P + \alpha[\text{DHO}]e^{-t/\tau_b}. \quad (16)$$

This equation was solved numerically using parameters appropriate for the situations described below. We have measured $\tau_b \sim 13$ s, [DHO] is the initial concentration of either 1 μM or 1 mM, and $\alpha = \beta/K_D$ where the K_Ds are known, hence the only unknown parameter in Eq. 16 is β so we computed a series of curves for different values of β until the model predicted the times for 63% recovery from blockade listed below.

The time course for removal of DHO blockade is not expected to be exponential, however the time for 63% recovery, $T_{.63}$, is a useful measure of the effect of β. The value of β_h for type-h pumps was estimated using Eq. 16 with the initial [DHO] = 1 μM and our measured value of

$$T_{.63} = 32 \pm 7\ s\ (n = 5)\ [\text{DHO}] = 1\ \mu\text{M}. \quad (17)$$

The value of β_l for type-l pumps was estimated by using 1 mM DHO to block total pump current, then changing the bath to a concentration of 5 μM DHO, so the type-h pumps remained blocked and the change in current reflected recovery of the type-l pumps only. From these experiments

$$T_{.63} = 88 \pm 12 \text{ s } (n = 5) \text{ [DHO]} = 1 \text{ mM}. \quad (18)$$

Using Eq. 16 with $\tau_b = 13$ s, we determine

$$\beta_h = 0.083 \text{ s}^{-1}$$
$$\beta_l = 0.017 \text{ s}^{-1}. \quad (19)$$

Given the standard deviations in our measured values of $T_{.63}$ and variability in the rate of bath exchange, the values of β in Eq. 19 have considerable uncertainity. To estimate their sensitivity, we assumed a range of 16 to 10 s for τ_b and bracketed the values of β at $0.059 \leq \beta_h \leq 0.143$ and $0.014 \leq \beta_l \leq 0.020$.

The values of α are determined from $K_{Dh} = \beta_h/\alpha_h$ and $K_{Dl} = \beta_l/\alpha_l$ and differ by three orders of magnitude.

$$\alpha_h = 1.1 \times 10^5 \text{ M}^{-1}\text{s}^{-1}$$
$$\alpha_l = 2.4 \times 10^2 \text{ M}^{-1}\text{s}^{-1}. \quad (20)$$

In summary, mammalian ventricular myocytes appear to have two types of Na/K pumps, with glycoside affinities differing by approximately two orders of magnitude, due in large part to different on-rates. DHO blockade of either type pump was not significantly affected by $[Na]_i$ or $[K]_o$. An increase in $[Na]_i$, increased both i_h and i_l by about the same amount without altering their respective K_Ds. A decrease in $[K]_o$ primarily caused i_l to decrease thus increasing the fraction of i_h/i_T, but the effect on the K_Ds was not sufficiently large to reliably detect.

$[Na]_i$ and $[K]_i$ Effects

Fig. 3 illustrates the dependence of pump current on $[Na]_i$ with $[K]_o = 4.6$ mM. The raw data in the upper two records in Fig. 3 *A* are total pump current measured at two different $[Na]_p$. The dashed lines represent our estimate of the change in current, determined from 15 to 30 s of data just before the onset of DHO blockade and 15 to 30 s of data during maximum blockade. The lowest $[Na]_p$ used to measure I_T was 3 mM, which gave an average current of 32 pA. For just the type-h pumps, the lowest $[Na]_p$ was 10 mM, which gave smaller currents as shown in the bottom panel of Fig. 3 *A*. For these small currents, baseline drift introduces significant uncertainty, however, the characteristic time course of DHO blockade helps to identify the pump associated change in current. Results were discarded if obvious shifts in baseline occurred during the course of the experiment. Otherwise, we assume small random shifts will average out with five or more independent measurements. Table II gives mean current and standard deviations for i_T and i_h at each value of $[Na]_p$. These data were obtained through a population study with each point representing the average from 5 to 10 different cells.

Fig. 3 *B* illustrates P_{Na} as a function of $[Na]_p$ (*lower curve*) or our estimate of $[Na]_i$ (*upper curve*). The value of $[Na]_i$ was calculated as described in Methods from Eq. 1 (also see the figure legend). The corrections shift the P_{Na} vs [Na] curve to the left and increase the steepness at the midpoint. The half-saturating value of [Na] shifted from 14 to 9.6 mM. For typical corrections, we estimate that $[Na]_p = 10$ mM yields $[Na]_i = 6.9$ mM whereas $[Na]_p = 50$ mM yields $[Na]_i = 36$ mM. However, the

effect on the value of current is not proportional to these changes. Assuming the upper curve in Fig. 3 *B* is our best estimate of $P_{Na}([Na]_i)$, the values are $P_{Na}(10)$ = 0.51 vs $P_{Na}(6.9)$ = 0.40, a significant effect, whereas $P_{Na}(50)$ = 0.86 vs $P_{Na}(36)$ = 0.82, a fairly minimal effect, which motivate our choice of $[Na]_p$ = 50 mM in many

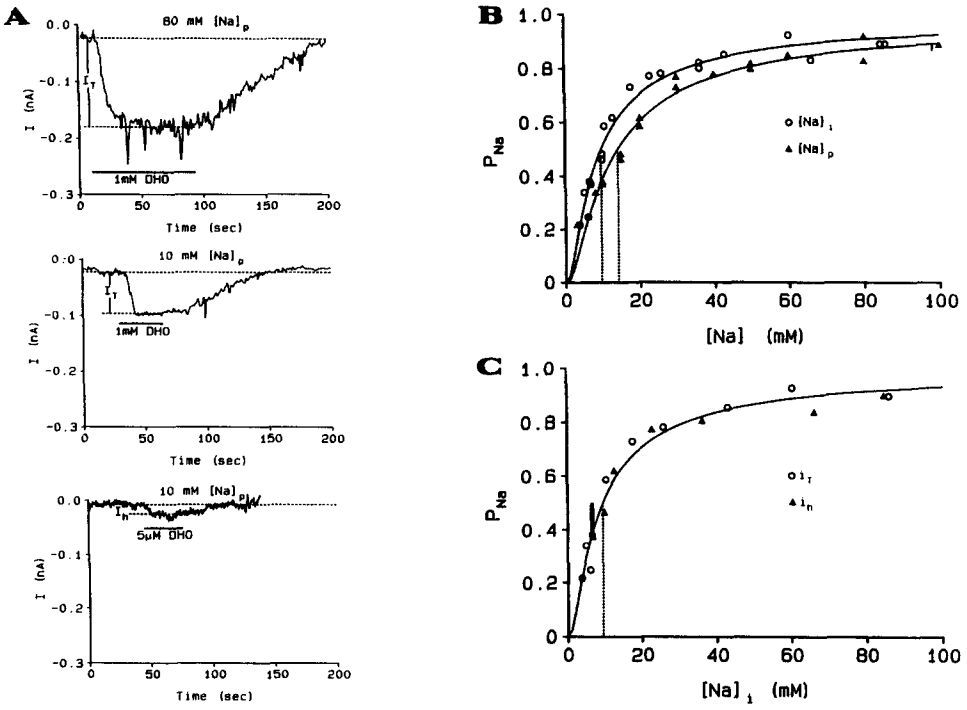

FIGURE 3. The dependence of the two types of Na/K pumps on $[Na]_i$. The data are recorded at $\psi_i = -60$ mV and $[K]_o$ = 4.6 mM. From these studies we conclude the $[Na]_i$ dependence of the two types of pumps is the same and neither type of pump is affected by $[K]_i \leq 140$ mM. (*A*) The protocol for measuring the $[Na]_i$ dependence of the two pumps. A population of 5 to 10 cells was studied at each value of $[Na]_p$. Total pump current was measured by blockade with 1 mM DHO with $[Na]_p$ varying from 3 to 100 mM. The high-affinity type pump current was measured by blockade with 5 μM DHO with $[Na]_p$ varying from 10 to 100 mM. (*B*) The original data in Table II and data corrected for shifts between $[Na]_p$ and $[Na]_i$; each point is the result of dividing the measured current by the projected value of current at infinite $[Na]_p$. The value of $[Na]_i$ was estimated as described in Methods around Eq. 1. The values of R_p, I_T or I_h were the averages recorded for the group of cells with a particular $[Na]_i$. For all experiments, average R_p = 4 MΩ with deviations of ±1 MΩ for specific $[Na]_i$. I_{ib} was estimated for each $[Na]_p$ by assuming i_{ib} = 0.75 μA/μF at $[Na]_i$ = 6 mM, multiplying by the average capacitance of the group of cells, then using Eq. 6 to adjust for the actual value of $[Na]_i$. The data are graphed as a function of $[Na]_p$ (*lower curve, triangles*) or $[Na]_i$ (*upper curve, circles*). Half-max values are indicated by the dashed lines. (*C*) A comparison of the $[Na]_i$ dependence of total pump current, i_T, and high-affinity type pump current, i_h, showing no difference in activation. The dashed line indicates half saturation at $[Na]_i$ = 9.6 mM for either type of pump. The heavy bar indicates a point where total pump current was measured at two different values of 140 and 70 mM $[K]_i$ without any significant difference, suggesting the dissociation constants for $[K]_i$ are much larger than 140 mM (normal $[K]_i$) so this step is not rate limiting to the cycle.

of our experiments. In addition to these steady state changes in $[Na]_i$, we estimated the effects of transient changes in $[Na]_i$ during the application of 5 μM DHO. This was thought to be necessary because during blockade of I_h the accumulation of intracellular Na^+ stimulates I_l and causes an underestimate of I_h. This effect turned out to be <5%, so we did not make the correction.

The data in Fig. 3 were usually recorded by replacing $[K]_p$ with $[Na]_p$, so the values varied from $[K]_p$ = 147 mM at $[Na]_p$ = 3 mM to $[K]_p$ = 50 mM at $[Na]_p$ = 100 mM. Nakao and Gadsby (1989) performed similar studies using very low resistance pipettes with $[K]_p$ = 0 mM and ψ_i = 0 mV. Nevertheless, their curve is remarkably similar to the curve in Fig. 3 *C*, suggesting neither ψ_i nor $[K]_i$ significantly affect the interaction of $[Na]_i$ with the pumps. We verified $[K]_i$ had no effect by measuring the point with the bar in Fig. 3 *C* at two values of $[K]_p$. With $[Na]_p$ = 10 mM, we substituted choline for potassium and determined

$$i_T = 0.36 \pm 0.11\ \mu A/\mu F\ (n = 7)\ \text{at}\ [K]_p = 140\ \text{mM}$$
$$i_T = 0.37 \pm 0.12\ \mu A/\mu F\ (n = 9)\ \text{at}\ [K]_p = 70\ \text{mM}. \quad (21)$$

This large reduction in $[K]_i$ had no effect, which implies the dissociation constants are significantly larger than $[K]_i$ = 140 mM. Thus, removal of intracellular K^+ is not rate limiting under normal physiological conditions.

Table II shows i_h is consistently 0.33 i_T, regardless of $[Na]_i$, which implies both i_l and i_h have the same dependence on $[Na]_i$. As described below, we fit a model to these data and obtained projections of i_T = 0.97 μA/μF and i_h = 0.32 μA/μF at $[Na]_i \rightarrow \infty$. These projections were used to normalize the data and generate the P_{Na} vs $[Na]_i$ curve shown in Fig. 3, *B* and *C*, where we lumped together the total and high DHO affinity data. Note the projected value of i_T is not the same as i_{max} in Eq. 12 because neither the $[K]_o$ dependence nor the pH_o effect is saturated in these conditions.

There is considerable evidence (reviewed in Glynn, 1988) for a 3 Na^+:2 K^+ stoichiometry. Thus, activation of current reflects binding of 3 Na^+s and most likely depends on three effective dissociation constants. However, to the accuracy of the data, a simpler model for three independent, identical binding sites is adequate. Viz,

$$P_{Na} = \left(\frac{[Na]_i}{[Na]_i + K_{Na}}\right)^3 \quad (22)$$

The half-saturating value of $[Na]_i$ is given by $K_{Nal/2}$ where $(2^{1/3} - 1)K_{Nal/2} = K_{Na}$. The data give

$$K_{Nal/2} = 9.6\ \text{mM} \quad (23)$$

which implies K_{Na} = 2.5 mM. An equation of the Hill-type, $[Na]_i^n/([Na]_i^n + K_{Nal/2}^n)$, with the same value of $K_{Nal/2}$ = 9.6 mM and n = 1.24 will generate a theory curve indistinguishable from that shown in Fig. 3 *C*. Thus, one should not equate a Hill coefficient with the number of ligands binding to a site (Wyman and Gill, 1990, section 2.5) and for the situation here, a Hill coefficient of 1.24 only implies a lack of cooperative binding. For comparison, Nakao and Gadsby (1989) fit their $[Na]_i$ acti-

vation data using the Hill equation and determined $K_{Nal/2}$ = 10 mM and n = 1.4. We could choose a model with three independent dissociation constants or vary $K_{Nal/2}$ and n in the Hill equation to slightly improve the fit, but the main points are as follows: (*a*) the activation of current is a saturable Michaelis-Menten type function of $[Na]_i$. (*b*) The data dictate a $K_{Nal/2}$ of 9–10 mM regardless of the model. (*c*) The data (either here or in Nakao and Gadsby, 1989) suggest independent sites for the three Na^+s rather than cooperative binding. And (*d*), the choice of a particular model requires more information than is available from these data.

In summary, the $[Na]_i$ dependence of the two types of pumps is the same, each having P_{Na} = 1/2 at $[Na]_i$ = 9.6 mM. Thus, each type pump is maximally sensitive to changes in $[Na]_i$ at concentrations in the normal physiological range. Conversely, neither type pump is affected by changes in $[K]_i$ between 0 mM and normal concentrations of ~140 mM. This implies the dissociation constants for intracellular-K^+, from the intracellular face of either type pump, are not rate limiting. Hence $[K]_i$ does not set or adjust the normal rate of transport, whereas $[Na]_i$ does.

$[K]_o$ *Effects*

Fig. 4 *A* illustrates the protocol for measuring the $[K]_o$ dependence of I_T or I_h. In all experiments we measured pump current in 8 mM $[K]_o$ and in a second test $[K]_o$; the order of the concentrations was random. The value of pump current determined in the test $[K]_o$ was divided by the value recorded in 8 mM, thus, removing cell to cell variability in membrane area or pump density. The average currents in 8 mM $[K]_o$ were

$$\begin{aligned} I_T &= 141 \pm 71 \text{ pA } (n = 21) \ [Na]_p = 50 \text{ mM} \\ I_h &= 42 \pm 13 \text{ pA } (n = 21) \ [Na]_p = 50 \text{ mM} \\ I_T &= 93 \pm 79 \text{ pA } (n = 15) \ [Na]_p = 10 \text{ mM}. \end{aligned} \tag{24}$$

When $[K]_o$ was changed, the holding current shifted, partly due to the change in K^+ conductance and K^+ equilibrium potential and partly due to the change in pump current. Because we measure the pump component by DHO blockade, changes in passive K^+ current do not affect our results.

Our method of using each cell as its own control (shown in Fig. 4 *A* and described in the last paragraph) greatly reduces the ratio of the standard deviation to mean current as can be seen by comparing the bars in Fig. 4, *B* and *C*, with the standard deviations in Eq. 24. However, data on relative activation are equal to unity at $[K]_o$ = 8 mM, which is not saturating. A theory curve was therefore generated, as described below, to project the $[K]_o$ activation to $[K]_o \to \infty$, which suggested activation at 8 mM $[K]_o$ is ~79% of saturation. The normalized data are the probability of $[K]_o$ activation of I_T, termed P_{KT}. Fig. 4 *B* compares $[K]_o$ activation of total pump current (I_T) measured at $[Na]_p$ = 10 mM with that measured at $[Na]_p$ = 50 mM. At each value of $[K]_o$, I_T is much larger with $[Na]_p$ = 50 mM than with $[Na]_p$ = 10 mM (see Eq. 24), but the normalized data show the activation curves are not different. One interesting conclusion from these data is $[K]_o$ activation of I_T is independent of $[Na]_i$, thus $[K]_o$ activation of both I_h (P_{Kh}) and I_l (P_{Kl}) must also be independent

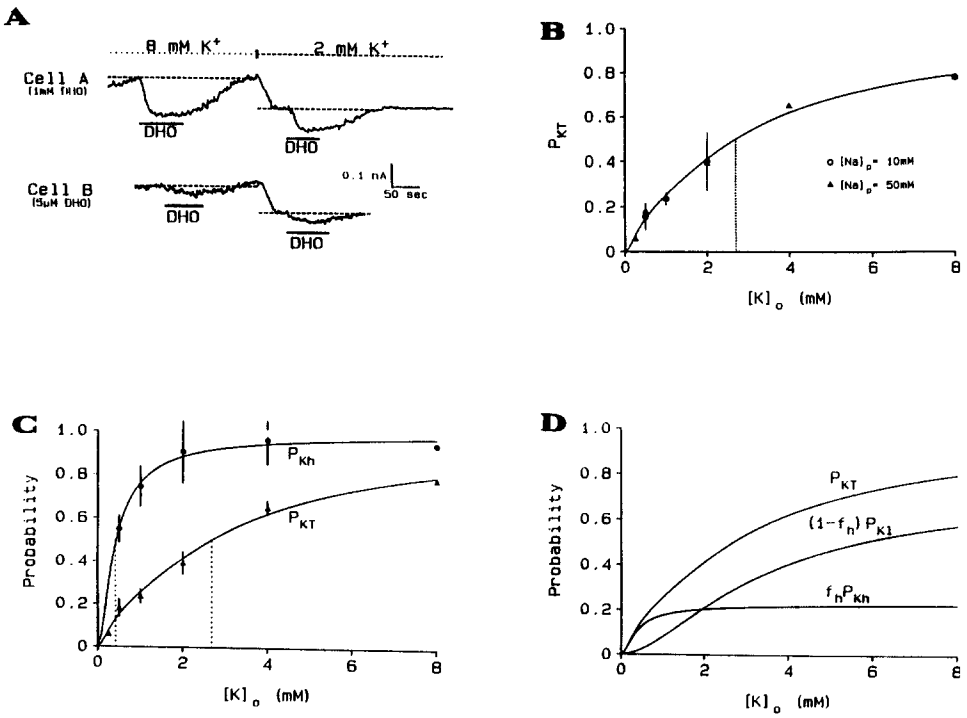

FIGURE 4. The dependencies of high- and low-affinity type pumps on extracellular potassium. The data were recorded at $\psi_i = -60$ mV and $[Na]_p = 50$ or 10 mM. The value of $[Na]_i$ had no significant effect on the $[K]_o$ dependence, however, the probability of modulating the high-affinity type pumps saturates at a much lower $[K]_o$ than for total pump current. (*A*) The protocol for measuring the $[K]_o$ dependence of total pump current (1.0 mM DHO) or high-affinity type pump currrent (5 μM DHO). We used 8 mM $[K]_o$ as our control condition in each cell and determined the current in a test $[K]_o$ relative to that in 8 mM. In general, the order of control and test $[K]_o$ was random and the data shown were chosen for convenience of presentation. When $[K]_o$ is changed, there is a change in baseline current partly due to the effect on K^+ conductance. DHO blockable current, however, reflects only the effect of $[K]_o$ on pump current. Nevertheless, in the period between the change in $[K]_o$ and the second application of DHO, the shift in pump current will have changed $[Na]_i$. For the data shown, $[Na]_p = 50$ mM so changes in $[Na]_i$ have negligible effect owing to saturation of the Na^+ activation curve. For the results where $[Na]_p = 10$ mM, we estimated the change in $[Na]_i$ and applied a small correction as described below. (*B*) Comparison of the $[K]_o$ dependence of total pump current at different values of $[Na]_i$. For the data recorded with $[Na]_p = 10$ mM, we estimated $[Na]_i$ using Eq. 4, assuming $I_T(t)$ followed the time course of the bath change ($\tau_b = 13$ s). For $[K]_o = 2$, 1, and 0.5 mM, we estimated $[Na]_i = 0.6$, 1.2, and 1.7 mM, respectively. The ratio of P_{Na} at$[K]_o = 8$ mM to P_{Na} at the test $[K]_o$ was 0.89, 0.81, and 0.75, respectively. The data shown are corrected mean values with the bars indicating standard deviations for the $[Na]_p = 10$ mM data. Standard deviations for the $[Na]_p = 50$ mM data are shown in *C*. (*C*) A comparison of $[K]_o$ activation of total and high-affinity type pump currents. These data were recorded at $[Na]_p = 50$ mM so corrections for changes in $[Na]_i$ were not considered necessary. We conclude the type-h pump current is activated by much lower values of $[K]_o$ than the total pump current. Assuming the total current is the sum of type-h and type-l currents, the type-l pump current must be activated by even higher concentrations of $[K]_o$ than is the total pump current. (*D*) The calculated activation of the two types of pumps with $[K]_o$ and how the two curves, P_{Kh} and P_{Kl}, combine to generate P_{KT}.

of $[Na]_i$. This observation is equivalent to writing the probability of $[K]_o$ activation and $[Na]_i$ activation for either I_h or I_l as a product ($P_{Na}\,P_{Kh,l}$) as we have done.

Fig. 4 *C* compares $[K]_o$ activation of I_T with that of I_h. Obviously, P_{Kh} saturates at a much lower $[K]_o$ than does P_{KT}. Our hypothesis is two types of pumps are expressed in these cells, hence P_{KT} is a composite function reflecting the weighted average of P_{Kh} and P_{Kl},

$$P_{KT} = f_h\,P_{Kh} + (1 - f_h)\,P_{Kl}$$
$$f_h = \frac{F_h}{F_h + (l - F_h)\,Q_h}. \tag{25}$$

Based on the data in Fig. 4, *B* and *C*,

$$P_{KT} = \frac{1}{2} \text{ at } [K]_0 = 2.6\text{mM}$$
$$P_{Kh} = \frac{1}{2} \text{ at } [K]_0 = 0.4\text{mM} \tag{26}$$

I_h becomes very small for values of $[K]_o$ less than 0.5 mM so we did not attempt to measure $[K]_o$ activation of I_h at these low $[K]_o$. As a consequence, the half-saturating $[K]_o$ is not very precisely determined, but it is clearly <1 mM.

The difference in $[K]_o$ activation at 5 μM vs 1 mM [DHO] is qualitatively what one would expect for $[K]_o$-[DHO] competition, however this interpretation is inconsistent with our [DHO] blockade data. For example, the DHO blockade data could only be interpreted as showing significant $[K]_o$-[DHO] competition if one assumed a single population of pumps, however, this is inconsistent with bimodal blockade that varies over four orders of magnitude of [DHO]. If we rule out a single population, then the DHO blockade data show competition must be small whereas the increase in i_h/i_T as $[K]_o$ is decreased implies the difference in $[K]_o$ activation shown in Figs. 4, *B* and *C*. Given the assumption of two pumps described by Eq. 25, P_{Kl} will be half-saturated at a value of $[K]_o$ greater than 2.6 mM. To determine the half-saturating $[K]_o$ for P_{Kl}, the data in Eq. 24 are used to determine f_h, then using the already determined curve for P_{Kh} we curve fit to P_{KT} to extract P_{Kl}. The fraction f_h is the ratio i_h/i_T at saturating $[K]_o$. From Eq. 24, at $[K]_o$ = 8 mM, I_h = 42 pA, which is saturated based on our P_{Kh} activation data, whereas at $[K]_o$ = 8 mM, I_T = 141 pA which is 79% of saturation, thus at saturation I_T = 78 pA. This yields

$$f_h = 0.24. \tag{27}$$

With f_h = 0.24, we curve fit to determine

$$P_{Kl} = \frac{1}{2} \text{ at } [K]_0 = 3.7 \text{ mM}. \tag{28}$$

The theory curve for P_{KT} was generated from Eq. 25 with P_{Kh} and P_{Kl} each being a second order (dependent on $[K]_o^2$) binding curve. However, a simple first order binding curve (Hill coefficient, n = 1.0) with half-saturation at $[K]_o$ = 2.6 mM generates an indistinguishable theory curve for P_{KT}. Nakao and Gadsby (1989) measured $[K]_o$ activation of total pump current in these cells at ψ_i = 0 mV and also con-

cluded the dependence was well fit by a first order binding curve, but their value of half-saturating $[K]_o$ was 1.5 mM rather than 2.6 mM as we have determined at $\psi_i = -60$ mV. They also measured the current-voltage relationship of total pump current at several $[K]_o$ and their data suggest a shift in P_{KT} to higher values of $[K]_o$ at hyperpolarized values of ψ_i. The data in Fig. 4 confirm the shift, suggesting $[K]_o$ activation has mild voltage dependence. Cohen et al. (1987) measured $[K]_o$ activation of total pump current at $\psi_i = -60$ mV in canine Purkinje cells and found half saturation at 0.8 mM $[K]_o$, which is more like the type-h pumps than type-l. These data, like the DHO blockade data, suggest the type-h predominates in Purkinje fibers whereas both type-h and type-l are important in ventricular myocytes.

The choice of a model for P_{Kh} and P_{Kl} was not critical; an equation for two independent binding sites, a Hill-type equation or the analysis below provided equally good fits and essentially the same conclusions. We assume activation of either type pump requires the binding of two extracellular K^+s, hence the activation curve for either type pump will have the form

$$P_K = \frac{[K]_0^2}{[K]_0^2 + K_{K2}[K]_0 + K_{K2}K_{K1}}. \tag{29}$$

Our analysis of the Albers-Post cycle (work in progress) suggests K_{K1} might be less than K_{K2}. Based on this and to simplify the analysis here we assume

$$\frac{1}{2}K_{K2} = K_{K1} = K_{K1/2} \tag{30}$$

where the values of $K_{K1/2}$ for P_{Kh} and P_{Kl} are reported in Eqs. 26 and 28.

Fig. 4 *D* shows the interaction of $[K]_o$ with the two different types of pumps and how we assume the two curves combine to generate the $[K]_o$ dependence of total pump current. In Fig. 4 *D*, note that when $[K]_o$ is below ~2 mM, the majority of the current is from the high DHO affinity pumps whereas at higher $[K]_o$ the majority is from the low-DHO affinity pumps. This implies the apparent affinity for DHO shifts from high affinity to low affinity as $[K]_o$ varies from <2 mM to its saturating value. In ventricle, some significant component of the apparent competition between $[K]_o$ and glycoside inhibition may reside in this difference in K^+ sensitivity of the two types of pumps.

In summary, $[K]_o$ activation and DHO blockade are associated with interactions at the extracellular faces of the two pumps whereas $[Na]_i$ acts at the intracellular faces, suggesting the major difference in these pumps resides in their extracellular domains. Normal physiological variations in $[K]_o$ would be unlikely to go sufficiently low to have a large effect on transport by the type-h pumps, however half-saturation of the type-l pumps occurs near the value of normal physiological $[K]_o$. Because these cells express a combination of these two types of pumps, i_h is able to maintain a significant level of Na/K transport at the lowest physiologically relevant values of $[K]_o$ while i_l responds vigorously to changes in $[K]_o$ over all physiologically relevant concentrations.

pH_O Effects

Fig. 5 *A* illustrates our protocol and the basic finding for acute effects of pH_o on I_h and I_T. For the record in Fig. 5 *A*, $[Na]_p$ = 50 mM and $[K]_o$ = 4.6 mM. We measure either I_h or I_T at pH_o = 7.4 in each cell, then in the same cell, change pH_o to a test value (here pH_o = 6.8), and remeasure I_h or I_T. In most experiments we were able to measure only I_h or I_T in a single cell, but Fig. 5 *A* illustrates one of a few instances

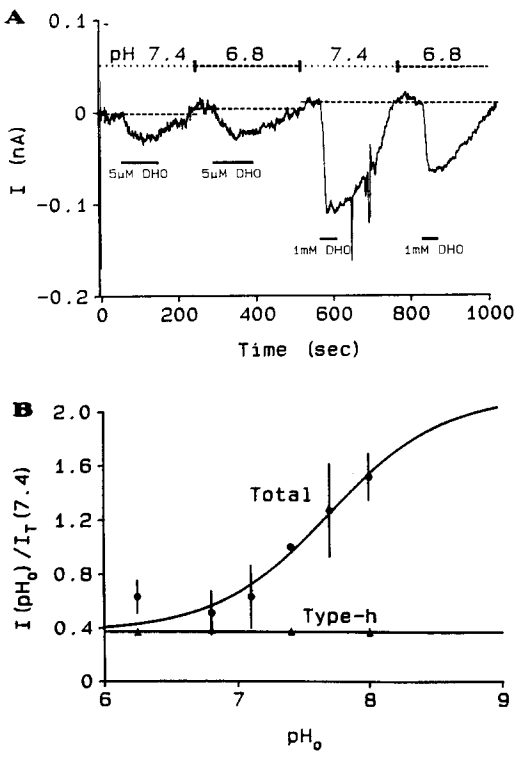

FIGURE 5. The dependencies of type-h and type-l pumps on extracellular pH. The data were recorded at ψ_i = −60 mV, $[K]_o$ = 4.6 mM and $[Na]_p$ = 10 or 50 mM, however, the value of $[Na]_p$ had no significant effect on the conclusions (see controls in text). The single record in *A* or the average responses in *B* show total pump current is significantly inhibited by $[H]_o$ whereas the type-h pump current is not, suggesting yet another functional difference insofar as the inhibition of i_T appears to result from an inhibition of i_l and not i_h. (*A*) An original time record illustrating that I_h (5 μM DHO) is not noticeably affected by changing pH_o whereas I_T (1 mM DHO) is, hence the proposal that pH_o affects I_l but not I_h ($I_T = I_h + I_l$). For this experiment, $[Na]_p$ = 50 mM. (*B*) Average responses with standard deviations of total pump current and type-h current as functions of pH_o. For each curve, the pump current was measured in the same cell at a test pH_o and a control pH_o = 7.4. The value of pump current at the test pH_o was divided by the value at pH_o = 7.4 to obtain the relative effect. For these curves, the total pump current was measured at $[Na]_p$ = 10 mM whereas the type-h current was measured at $[Na]_p$ = 50 mM. The two curves were scaled such that i_h is 0.37 i_T at pH_o = 7.4 (see text for justification). The scaled value of i_T as $[H]_o \rightarrow 0$ is projected to go to a value 2.34 times greater than its value at pH_0 = 7.4 whereas it is constrained as $[H]_o \rightarrow \infty$ to go to 0.37 its value at pH_0 = 7.4. This implies i_l will increase three-fold as pH_o goes from 7.4 to infinity and i_l will decrease to zero as pH_o goes very acid. When pH_o is changed, i_l changes and thus $[Na]_i$ changes. For data recorded with $[Na]_p$ = 10 mM the effect of a change in $[Na]_i$ can be significant, hence we made corrections. At $[Na]_p$ = 10 mM, for these cells we estimated from Eq. 1 that the average $[Na]_i \simeq 8.5$ mM. The maximum changes in $[Na]_i$ were $< \pm 2$ mM as estimated from Eq. 4. The ratio of P_{Na} evaluated at pH_o = 7.4 to its value at the test pH_o of 6.25, 6.8, 7.1, 7.7, and 8.0 was 0.90, 0.88, 0.94, 1.07, and 1.18 respectively. The raw data were multiplied by these ratios to obtain the corrected total pump curve in *B*.

in which we measured both. The value of I_h is small and subject to some uncertainty, but even in this single record there appears to be little effect of pH_o on I_h whereas there is clearly a large effect on I_T, suggesting I_l is inhibited by reducing pH_o. Fig. 5 *B* illustrates average values (and standard deviation) for normalized I_h at various pH_o under the same conditions ($[Na]_p$ = 50 mM and $[K]_o$ = 4.6 mM). The averages bear out the initial impression that pH_o does not significantly affect I_h, at least not in this time period. These data address only acute effects of pH_o and other long term effects may occur.

The dependence of I_T on pH_o shown in Fig. 5 *B* was recorded at near normal physiologic conditions of $[Na]_p$ = 10 mM and $[K]_o$ = 4.6 mM. As described in the legend, a small correction was made for changes in $[Na]_i$ induced by the change in pH_o. If we treat I_T as a function of $[H]_o$ so $I_T(0)$ is $I_h + I_l$ at $[H]_o = 0$, where no current is blocked by H^+, and $I_T(\infty)$ is $I_h + I_l$ at $[H]_o \to \infty$. The form of the equation used to fit the data is

$$I_T([H]_0) = I_T(\infty) + [I_T(0) - I_T(\infty)]Q_H \tag{31}$$

where Q_H is defined in Eq. 11 and represents the fraction of type-l pump current not blocked by extracellular H^+. Physically, this model implies one H^+ binds to each type-l pump and reduces its rate of turnover. If H^+ reduces type-l turnover to zero as $[H]_o \to \infty$, then $I_T(\infty) = I_h$. The data on $I_T([H]_o)$ in Fig. 5 *B* provide just a segment of the binding curve since values of pH_o less than 6.25 or greater than 8.00 caused irreversible cell damage. Thus, the model in Eq. 31 is a first approximation and the projections to zero or infinite $[H]_o$ are not experimentally justified. Nevertheless, an estimate of $I_T(0)$ is of interest since it allows us to estimate the maximum current generated by type-l pumps. At very acid pH_o, the data in Fig. 5 *B* are not inconsistent with $I_T(\infty) = I_h$, so we make this assumption. With $[K]_o$ = 4.6 mM and pH_o = 7.4, we have estimated previously that I_h/i_T is between 0.3 and 0.4. The fit to the data in Fig. 5 *B* is statistically slightly better at the high end of this range, and since the fraction 0.37 was obtained from the DHO data, we set

$$I_T(\infty) = I_h = 0.37\, I_T\,(pH_o = 7.4)\,. \tag{32}$$

This assumption yields

$$Q_H = \frac{1}{2} \quad \text{at} \quad pH_o = 7.4, \tag{33}$$
$$K_H = 19 \text{ nM}.$$

Thus, we estimate that $Q_H \simeq 0.32$ at pH_o = 7.4 so I_l is normally at 32% of its maximum value.[1] This implies I_T is at 43% of its maximum or, as $[H]_o \to 0$, I_T can increase by a factor of 2.34 over its value at pH_o = 7.4.

Breitweiser, Altamirano, and Russel (1987) reported Na/K pump current in squid axon was modulated by intracellular pH_i. In the whole-cell patch configuration, we buffer pH_i so it is unlikely to change when pH_o changes, nevertheless, the

1. If we use the Table II estimate that $I_h = 0.33\, I_T$ at pH_o = 7.4, the best fit K_H = 23 nM and Q_H = 0.37 at pH_o = 7.4.

effect of pH_i on I_T is of interest so we performed the following experiments. Pipettes containing intracellular solutions with 6 mM $[Na]_p$ and pH_i buffered to 6.0 or 7.2 were used. After the patch was made and the underlying membrane ruptured, we waited at least 5 m for the pipette and intracellular solutions to equilibrate. The capacitance of each cell was measured, then 1 mM DHO was used to determine I_T. We normalized and averaged the results from the two populations of cells to obtain (mean ± SD).

$$i_T = 0.23 \pm 0.03\ \mu A/\mu F\ (N = 8)\ pH_i = 6.0$$

$$i_T = 0.24 \pm 0.06\ \mu A/\mu F\ (N = 8)\ pH_i = 7.2. \tag{34}$$

Moreover, as the pH = 6.0 pipette solution diffused into the cell, there were significant effects on membrane currents other than the pump. The time constant for intracellular equilibration (~100 s) was about the same as we determined when pipette K^+ diffused into these cells, suggesting this is the time constant for the contents of the pipette to come to a diffusional steady state with the cell (Mathias et al., 1990). Given this slow time constant, it was possible to measure I_T at near normal pH_i during the initial 50 s after the rupture of the patch membrane, then in the same cell, measure I_T at $pH_i = 6.0$ after ~5 m. We do not precisely know the normal value of pH_i though we expect it to be much higher than 6.0. The ratio in four cells was

$$\frac{I_T(\text{normal } pH_i)}{I_T(pH_i = 6.0)} = 1.00 \pm 0.03. \tag{35}$$

Thus, pH_i appears not to affect either type of Na/K pump in these cells. We next performed a series of control experiments to rule out indirect effects of pH_o, possibly through causing changes in $[Na]_i$ or the K^+ concentration in the t-system lumen. These experiments also address the possibility that pH_o alters I_1 by changing its $[Na]_i$ or $[K]_o$ activation curve.

One concern was changing pH_o might alter $[Na]_i$, possibly through Na/H exchange, and thus indirectly change I_T. However, the data in Fig. 5 *A* were recorded at $[Na]_p$ = 50 mM whereas the total pump data in Fig. 5 *B* were recorded with $[Na]_p$ = 10 mM, yet both show significant inhibition of I_T at acid pH_o. We performed a series of experiments and found that

$$\frac{I_T(6.8)}{I_T(7.4)} = 0.64 \pm .10\ (n = 11) \quad \text{at} \quad [Na]_p = 50\ \text{mM} \tag{36}$$

whereas in Fig. 5 *B*

$$\frac{I_T(6.8)}{I_T(7.4)} = 0.53 \pm .14\ (n = 8) \quad \text{at} \quad [Na]_p = 10\ \text{mM}. \tag{37}$$

Given Eqs. 36 and 37 represent different populations of cells from different batches of animals and the data were recorded at different times, the ratios are probably not significantly different. Clearly, regardless of $[Na]_i$, a reduction in pH_o

significantly inhibits the pump current, suggesting the pH_o effect is not secondary to a change in $[Na]_i$. In addition, we looked at the inward background Na^+ current at $pH_o = 6.8$ and 7.4 using the method shown in Fig. 1 *A*. The results from eight cells were

$$\frac{I_{ib}(6.8)}{I_{ib}(7.4)} = \frac{205 \pm 93 \text{ pA}}{206 \pm 97 \text{ pA}}. \tag{38}$$

These results suggest the pH_o effects are not via changes in $[Na]_i$, and moreover, since inhibition occurs when $[Na]_i$ is saturating, the mechanism of inhibition is not by changing the affinity for $[Na]_i$.

As described in the Appendix, changes in t-system K^+ concentration are expected to be small, nevertheless, we measured the effect of pH_o with high $[K]_o$ and determined

$$\frac{I_T(6.8)}{I_T(7.4)} = \frac{54 \pm 15 \text{ pA}\,(N = 16)}{93 \pm 79 \text{ pA}\,(N = 15)} = 0.58 \text{ at } [K]_o = 8 \text{ mM}. \tag{39}$$

Though these were different groups of cells, the inhibition at acid pH_o still occurs when $[K]_o = 8$ mM, thus the effect of pH_o is unlikely to be due to changes in t-system K^+ concentration.

One mechanism for pH_o to affect I_l could be through changing the affinity for $[K]_o$. However, one has to be careful in testing for a shift in affinity since even our model (Eq. 12) predicts changes in P_{KT} when pH_o is changed (f_h depends on pH_o, see Eqs. 25 and 12). If the reduction in I_l as pH_o is changed from 7.4 to 6.8 were due to a shift in K^+ affinity, the value of half-saturating $[K]_o$ would have to shift from 3.7 to 11.3 mM. Such a shift would imply the midpoint of P_{KT} would shift by 5.11 mM to higher $[K]_o$. In contrast, if pH_o is only affecting f_h, the midpoint of P_{KT} would shift by 1.17 mM to lower $[K]_o$. We measured an abbreviated version of P_{KT} at $pH_o = 6.8$ and compared it to the raw data for P_{KT} given in Fig. 4. Curve fits to the two data sets suggested the midpoint of P_{KT} shifts by 0.54 mM to lower $[K]_o$ as pH_o is changed from 7.4 to 6.8. This is reasonably consistent with our model and completely inconsistent with a shift in $[K]_o$-activation.

Since we measure I_T as the current blocked by 1 mM [DHO], another possible mechanism for the effect of pH_o is to alter DHO binding. If so, then based on the data in Fig. 5 *B*, reducing pH_o from 7.4 to 6.8 will reduce DHO blockade of I_T from 96 to 51%. We tested this by measuring the ratio of currents blocked by 1 and 2 mM DHO at $pH_o = 6.8$. In five cells,

$$\frac{I_T\ ([DHO] = 1 \text{ mM})}{I_T\ ([DHO] = 2 \text{ mM})} = 0.99 \pm .03 \text{ at } pH_o = 6.8. \tag{40}$$

Thus, 1 mM DHO is still essentially saturating at $pH_o = 6.8$ and the pH_o effect is not through altered DHO binding.

In summary, the type-l pumps are inhibited by acid pH_o whereas the type-h are not. Neither type of pump is affected by a change in pH_i. This represents another

functional difference in the two types of pumps and again, the difference appears to be in the extracellular domain of the enzymes.

Summary of Results

The data presented here, taken in total, suggest the two-pump model previewed in Eq. 12. With $[Na]_i = 6$ mM, $[K]_o = 4.6$ mM and at $\psi_i = -60$ mV, $i_T \simeq 0.25$ μA/μF and I_h is between 30 and 40% of i_T. Based on these values and assuming the same maximum turnover rate for each type of pump we can estimate i_{max} and F_h, thus completing a quantitative description of Eq. 12, which is summarized here. The larger value of i_{max} corresponds to the smaller fraction F

$$\begin{aligned} i_T &= i_{max} P_{Na} [F_h P_{Kh} + (1 - F_h) P_{kl} Q_H] \\ i_{max} &\approx 2.88 \text{ to } 2.56 \ \mu A/\mu F \\ F_h &\cong 0.08 \text{ to } 0.12 \\ P_{Na} &= \frac{1}{2} \text{ at } [Na]_i = 9.6 \text{ mM} \\ P_{Kh} &= \frac{1}{2} \text{ at } [K]_o = 0.4 \text{ mM} \\ P_{Kl} &= \frac{1}{2} \text{ at } [K]_o = 3.7 \text{ mM} \\ Q_H &= \frac{1}{2} \text{ at } pH_o = 7.7 . \end{aligned} \tag{41}$$

The predictions of Eq. 41 with $F_h = 0.10$ are graphed in Fig. 4 *D* and are reasonably consistent with direct measurements of the fraction of type-h pump current Viz

$[K]_o$	=	1.0	4.6	8.09	mM	
i_h/i_T		0.69	0.34	0.29	Theory (see Fig. 4D)	
i_h/i_T		0.48	0.37		DHO-blockade	(42)
i_h/i_T			0.33		$[Na]_i$-activation	
i_h/i_T				0.29	$[K]_o$-activation.	

The largest discrepancy is at 1 mM $[K]_o$, where the current is smallest and most difficult to accurately measure. Moreover, the analysis contains some uncertainty. Clearly, there is qualitative agreement that increasing $[K]_o$ decreases the fraction of i_T contributed by the high-DHO affinity pumps.

DISCUSSION

The main conclusion from this work is functionally different types of Na/K pumps exist and can be coexpressed in the same cell. Thus, each tissue has the ability to express a unique mix of pump types and consequently possess a unique total pump current which is in some way optimized for tissue function. As we noted in the Introduction, Na/K pump current is an important determinant of the cardiac action potential, which varies significantly from region to region of the heart. Na/K

pumps may therefore need to be specialized, just like ion channels, in order to generate the different action potentials. Our results demonstrate specialization is possible, and moreover, DHO blockade and $[K]_o$ activation of current in canine Purkinje cells is similar to that of the high affinity type pump (Cohen et al., 1987) whereas in ventricle both types are important, so specialization seems likely.

In these ventricular myocytes, the $[Na]_i$ activation curve for both types of pumps is set to respond to changes in Na^+ influx. However, given the cell volume and magnitude of pump current reported here, changes in $[Na]_i$ are slow relative to the duration of the action potential. We estimate time constants of minutes, which agrees with experimental observations by Cohen et al. (1987) who reported changes in $[Na]_i$ in canine Purkinje cells occurred with a time constant of 1.5 m. In such a time frame, many action potentials are generated in a normal heart so there is essentially no beat to beat modulation of $[Na]_i$. Rather, as action potential frequency changes, causing a change in the average inward sodium flux, $[Na]_i$ will slowly change and thus alter Na/K pump current. Though the response time is slow, the gain of the feedback system is fairly high and we calculate from the slope around normal $[Na]_i$ that the Na/K pumps limit the change in $[Na]_i$ per change in a cell's Na^+ influx to ~0.08 mM/pA. In other words, if I_{ib} increased by an average of 1 pA per cell, $[Na]_i$ would have to increase by 0.08 mM to cause an increase of 1 pA per cell in Na^+ efflux by the pumps.

The $[K]_o$ activation curve for type-l pumps (and thus total pump current) suggests a role in regulation of $[K]_o$, which is known to change with heart rate (Attwell, Cohen, and Eisner, 1981). In ventricle, the extracellular volume is smaller than intracellular, a factor which speeds up the effect of pump current on $[K]_o$, but the activation curve is less steep than that for $[Na]_i$, a factor that slows down the response. The net result is again Na/K pump regulation of $[K]_o$ will be slow relative to action potential duration and no beat to beat regulation occurs. We calculate the change in $[K]_o$ per change in K^+ efflux per cell is ~0.08 mM/pA, based on the response of the total Na/K pumps to small variations in $[K]_o$. In this case, if the background K^+ current per cell increased by an average of 1 pA, $[K]_o$ would have to increase by 0.08 mM for K^+ influx through the Na/K pumps to compensate.

The effect of pH_o on type-l pump current is more of an enigma. The H^+ blockade at normal $pH_o = 7.4$ is near the steepest part of the curve, so Na/K pump current is set to respond to changes in pH_o. However, if the extracellular spaces acidify, pump current is inhibited, $[Na]_i$ increases causing Na^+/H^+ exchange to be inhibited, thus allowing the intracellular space to also acidify. This seems backwards. There are apparently more complex interactions with transport systems which have not been considered here. Type-l pumps are dominant in ventricular muscle but nearly absent from Purkinje cells, thus the H^+ effects may have a role in the contraction cycle, a role that is not yet understood. Moreover, our model implies extracellular H^+ binds to type-l pumps and blocks their activity, but we have not tested for a shift in voltage dependence or in their affinity for extracellular Na^+, so this interpretation may be premature. Clearly, the role and mechanism of pH_o effects on I_l are interesting and require more experiments to elucidate.

The molecular basis of the two types of pumps in guinea pig ventricle is not known. The dissociation constants for DHO blockade of the type-h and type-l

pump currents correspond with DHO binding to the α2 (or α3) and α1 isoforms respectively. In most mammalian ventricular cells, α1 and α2 isoforms have been identified (by specific antibodies: Sweadner, Herrera, Amato, Moellmann, Gibbons, and Repke [1994] or Maixent, Charlemagne, Chapelle, and Lelievre [1987] by mRNA content: Gick, Hatala, Chon and Ismail-Beigi [1993]). Berrebi-Betrand, Maixent, Guede, Gerbi, Charlemagne, and Lelievre [1991] suggested α1 and α2 are present in guinea pig ventricle based on separating two α-subunits by molecular weight and glycoside affinity. However, Sweadner et al. (1994) using a specific antibody that detected α2 in guinea pig brain, was unable to detect α2 in guinea pig ventricle. Moreover, whereas [^{3}H] ouabain binding in canine or rat ventricle has two affinities (Maixent et al., 1987, Akera, Ng, Hadley, Katano, and Brody, 1986; Grupp, Grupp, and Schwartz, 1981); Hagane, Akera, Stemmer, Yao, and Yoroyama (1988) and Herzig and Mohr (1984) found only a single binding site in guinea pig ventricle. Glycoside blockade of Na/K pump current from isolated ventricular cells has now been measured in dog, guinea pig (Mogul et al., 1989) and rat (Berlin et al., 1992) with very consistent results. Thus, the presence of two functionally different Na/K pumps may be a general property of the mammalian ventricles. The difference in glycoside blockade of the type-h and type-l pump current suggests the α2 and α1 isoforms are the molecular basis and this is strengthened by the observation of primarily type-h current in canine Purkinje cells (Cohen et al., 1987), which have predominantly the α3 isoform (Zahler et al., 1992, 1993). However, the failure of a specific α2 antibody to bind in guinea pig ventricle (Sweadner et al., 1994) and the single ouabain binding site (Hagane et al., 1988; Herzig and Mohr, 1984) suggest we should not jump to conclusions. The evidence for α1 and α2 is correlative and therefore not compelling. It is possible the β-subunit isoform or a post-translational modification of the α-subunit causes the separation into two functional classes of pumps. On the other hand, the antibody used by Sweadner et al. (1994) might have failed to recognize the ventricular α2 or perhaps there is simply too little of the α2 in ventricle to be detected over nonspecific binding of either the antibody or [^{3}H]-ouabain. Assuming the two types of pumps have the same max turnover rate, we estimated that as little as 8% of the total pump proteins might be the type-h whereas, at physiological conditions, as much as 40% of the current might be generated by the type-h pumps. Hence, functional importance does not necessarily correlate with quantity of protein. More studies on the molecular basis of the two functionally different pumps are needed to decide this issue.

Critical Comparison of Results

Before addressing results of others, one should consider the limitations of in vivo studies. The Na/K pumps depend on multiple variables, those identified in these cells (Gadsby and Nakao [1989] Nakao and Gadsby [1989] and Gao et al. [1991]) are $[Na]_i$, $[K]_o$, ψ_i, $[Na]_o$, pH_o, $[Ca]_i$, and phosphorylation. To study the effect of any one of these, the rest should be maintained constant, a feat not possible at this time. The whole-cell patch-clamp of isolated single cells is probably the best technique for controlling these multiple variables, but as analyzed in Mathias et al. (1990) and demonstrated in this paper, changes in $[Na]_i$ remain a persistent problem.

DHO Binding

Daut and Rudel (1981) first measured DHO blockade of pump current in guinea pig ventricle using microelectrodes and pieces of syncytial tissue. They reported a single site with half-maximum blockade at [DHO] = 46 μM when $[K]_o$ = 3 mM. Many variables are poorly controlled in studies of intact syncytial tissue, hence we are not sure which, if any, could smooth a composite binding curve and make it appear like a single site. On the other hand, one could argue that our enzymatic dissociation of the cells modified some fraction of the pump molecules and artifactually created two classes of pumps. We tend to believe in the two sites since: (*a*) in canine Purkinje tissue, cells isolated using the same technique have only the high-affinity site; and (*b*) the K_D measured by Daut and Rudel (1981) is in the middle of our binding curve, so if our isolation procedure artifactually shifts the K_Ds, some pumps would have to shift to higher affinity while others to lower, an effect that seems unlikely.

Mogul et al. (1989) first reported Na/K pump current blockade occurred with two DHO affinities in guinea pig myocytes. Their blockade curve is similar to ours and their best fit values of K_{Dl} = 65 μM and i_h/i_T = 0.40 compare well with K_{Dl} = 72 μM and i_h/i_T = 0.37 reported here. However, our value of K_{Dh} = 0.75 μM differs significantly from the 0.05 μM reported by them. They performed a population study whereas we looked at relative blockade in the same cell, so our data have intrinsically less variance, which is a particular problem at the low concentrations of DHO where the current blocked is small. Moreover, they argued that changes in $[Na]_i$ were not significant but we are not so certain. Indeed, if we did not correct for changes in $[Na]_i$ our DHO binding curve would have had a more pronounced dip in the middle and the K_Ds would appear to be farther apart. A more precise value of K_{Dh} will likely require new technology for isolating, cloning, and expressing each pump in a simpler system.

Stimers et al. (1990, 1991) using the same whole-cell patch-clamp technique, report $[Na]_i$ significantly affects glycoside binding in embryonic chick heart cells whereas our results show no such effect. Thus, a critical comparison seems important. In this instance, control of $[Na]_i$ is of particular importance since lack of control would lead to the conclusion expressed in their paper, even if glycoside binding is independent of $[Na]_i$. For example, if we consider the worst-case situation where the pipette has no influence on $[Na]_i$, then as a nonsaturating concentration of ouabain binds and blocks part of the pump current, $[Na]_i$ would increase at some rate determined by the density of pumps in the membrane and the cell surface to volume ratio. If this rate is sufficiently rapid in comparison to the binding kinetics of ouabain, the unblocked current may increase at nearly the same rate as blockade and the total current thus remains at a constant value determined by the inward background sodium current. One would therefore detect essentially no blockade of current when the initial $[Na]_i$ is well below saturation, hence the apparent $K_{1/2}$ would seem to be infinite. Owing to the small volume of the chick cells, changes in $[Na]_i$ can occur very rapidly compared to the time course of the ouabain blockade, so such changes are feasible if the pipette does not control $[Na]_i$. Using Eq. 1 to calculate changes in $[Na]_i$, then for a single cell with 3 pA of pump

current being blocked, and pipette resistances from 10 to 20 MΩ (as reported in Stimers et al., 1991), $[Na]_i$ would have increased by 1 or 2 mM. This change in $[Na]_i$ is too little to produce their observation but sufficient to cause the apparent $K_{1/2}$ to approximately double. They report, however, their currents are from clusters of one to three cells. Given that patch clamp of one cell imperfectly controls $[Na]_i$, control of $[Na]_i$ in a second or third cell, with additional access resistance from one or two gap junctions, will be much worse. Thus, we believe their results are inconclusive. We report no significant effect of $[Na]_i$ on DHO binding but our results also have limitations, owing to the composite binding curve for our cells. Even a simple binding curve with variance in the data for percent bound yields considerable uncertainty in the best fit $K_{1/2}$. For a composite binding curve with more fit parameters the uncertainity is obviously increased, so we cannot rule out some effect of $[Na]_i$ on K_{Dl} and/or K_{Dh}. However, we do not believe changes in $[Na]_i$ have systematically biased our results since: (*a*) we avoid using cell pairs, which are visually obvious because of the regular geometry of our cells; (*b*) in our system the blockade of pump current by DHO is rapid compared to the time for changes in $[Na]_i$, hence control by the pipette is not so critical and the changes are kept small by the short exposure to DHO; and (*c*) we estimate the change in $[Na]_i$ from the observed time course of the blockade and make a correction to remove the majority of the artifact.

There is a large literature describing competition between $[K]_o$ and glycoside binding (reviewed in Eisner and Smith, 1991). These and other data have led to the hypothesis that glycosides bind to the phosphorylated E_2 configuration, with preference for the subset of states that interact with $[Na]_o$. In this model, increasing $[K]_o$ pulls the cycle out of the $[Na]_o$-binding states, thus increasing the K_D for the glycoside by a type of kinetic competition. The data in Figs. 2 and 4 illustrate another type of interaction between $[K]_o$ and glycoside affinity: as $[K]_o$ is increased, the fraction of total pump current contributed by the low-glycoside affinity pumps increases, causing the half-saturating concentration of glycoside for total pump current to shift to the higher concentrations necessary to block the low-affinity pumps. Given about a 100-fold difference in glycoside affinity between type-h and type-l pumps, one would observe nearly a 100-fold shift in the [DHO] at which $P_{DT} = 1/2$ as $[K]_o$ goes from very low to saturating values. The competition between $[K]_o$ and ouabain reported previously in ventricular tissue (e.g., Daut, 1983) could be entirely due to this shift phenomenon. In studies of other cells (Sachs, 1974; Stimers et al., 1991) we do not know whether two types of pumps were present, but it seems unlikely all of the reports of competition could be accounted for by two pumps. More likely, kinetic competition exists but quantitive data may include some of the shift effect. Another complication arises because, as $[K]_o$ increases, pump current increases and $[Na]_i$ drops. This results in a nonsaturating concentration of glycoside blocking a smaller fraction of total current when $[K]_o$ is elevated. To understand this problem, consider an extreme example. Assume $[K]_o = 1$ mM, and $[Na]_i = 25$ mM, which is essentially saturating. A half-maximal dose of glycoside will block half the pumps and cause $[Na]_i$ to increase further, but this will not affect the unblocked pumps whose dependence on $[Na]_i$ is saturated. We then increase $[K]_o$ to 6 mM, which further stimulates the pumps and causes $[Na]_i$ to drop to ~10 mM

where $[Na]_i$ activation is around one half. Assume the same concentration of glycoside still blocks half the pumps, allowing $[Na]_i$ to increase to near saturating hence unblocked pumps nearly double their turnover rate. It therefore appears the same concentration of glycoside blocks very little current. This artifactual competition depends on initial conditions, size of cell, rate of change of $[Na]_i$ and rate of action of glycoside, so it is difficult to estimate the extent of problems in experiments by others. However, the tendency will always be for higher $[K]_o$ to require a higher glycoside concentration to block the same fraction of pump activity, so one must arrange conditions to minimize the artifact. Glycoside blockade of in vitro ATPase activity is affected by [Na] and [K] (Inagaki, Lindenmayer, and Schwartz, 1974) but in these conditions the concentrations are not affected by turnover rate. Thus, these studies provide the best evidence for kinetic competition, however, it is difficult to extrapolate these results to the intact cells since kinetic competition depends critically on the state of the pumps. We attempted to detect kinetic competition by measuring [DHO] blockade curves at different $[K]_o$ (see Fig. 2 *C*). However, as previously noted, the presence of a composite binding curve makes it difficult to detect reasonably small shifts in the K_Ds, especially when the fraction of current contributed by the type-h pumps is obviously changing with $[K]_o$. Adequate fits to the data were obtained without allowing any changes in the values of K_{Dh} and K_{Dl}. We therefore suggest kinetic competition might be less than previously thought, but our data are not inconsistent with changes in the K_Ds up to a factor of 2. Again, we have taken care to avoid systematic artifacts due to changes in $[Na]_i$.

$[Na]_i$ Activation

The $[Na]_i$-activation curve measured at $\psi_i = -60$ mV and several $[K]_i$ (Fig. 3) is very similar to that reported by Nakao and Gadsby (1989) for these same cells, but measured at $\psi_i = 0$ mV and $[K]_i = 0$ mM. Our $[Na]_i$ activation curve was corrected from an original half-maximum activation at 14 mM to our best estimate of 9.6 mM, a correction of 4.4 mM. Nakao and Gadsby (1989) report their pipette tips are 5 μM in diameter, which is significantly larger than the diameter of the pipette tips used in our studies. Nevertheless, small differences between $[Na]_i$ and $[Na]_p$ are inescapable. To the accuracy of the data in these two studies, however, we conclude the results agree and estimate half-maximum activation occurs at $[Na]_i$ between 9 and 10 mM, and is independent of membrane voltage, $[K]_i$, and $[K]_o$.

$[K]_o$ Activation

Our $[K]_o$ activation curve for total pump current is very similar to that measured by Nakao and Gadsby (1989) though the comparison is complicated by differences in protocol. In Fig. 4 *B* we graph total pump current vs $[K]_o$ at $\psi_i = -60$ mV and find half-saturation at 2.6 mM. Nakao and Gadsby (1989) measure total pump current vs $[K]_o$ at $\psi = 0$ mV and find half-saturation at 1.5 mM, then measure the ψ_i dependence at several $[K]_o$. From their total pump current vs ψ_i data, it appears activation by $[K]_o$ requires higher concentrations as the cell is hyperpolarized; at −60 mV, half-maximum activation appears to be very nearly at $[K]_o = 2.6$ mM. Thus, we believe our data agree with the results of Nakao and Gadsby (1989) though our two-pump interpretation is different.

pH Effects

There have been many studies demonstrating ATPase activity of isolated Na/K pumps has a maximum around normal physiological pH (discussed in Breitweiser et al., 1987). In addition, lowering pH_o, with pH_i not monitored or controlled, has been reported to inhibit Na/K pump activity in skeletal muscle (Keynes, 1965) and red blood cells (Beauge and Adragna, 1974), but the site of action was not certain. Lowering intracellular pH caused inhibition of the Na/K pumps in squid axon (Breitweiser et al., 1987) and barnacle muscle (Russel et al., 1983). We have found intracellular pH has no effect (in the range of 6.0–7.2) on Na/K pumps from guinea pig ventricular myocytes whereas lowering external pH (in the range 8.00–6.25) specifically inhibits the type-l pumps. We do not know the reasons for these differing results, however, as described below there are some differences in conditions of the experiments. In contrast to studies of isolated pump preparations, we specifically change pH on one side of the pump and maintain the pump at a -60 mV potential in an assymetric ionic environment. These differences in experimental conditions could account for differences in results, particularly since we can only alter pH over a limited range and still maintain a living cell. The specific pH_i effects mentioned above were recorded from marine animals, whose Na/K pumps work in a very different environment from those of land animals, hence there are bound to be differences in sensitivity to ionic environment. In the heart there are relatively high levels of metabolic activity, which is continuously changing, so variations in both intracellular and extracellular pH are expected. Thus, we believe the dependence of type-l pumps on pH_o and not pH_i has a specific physiological function.

Summary

Our observation that two functionally different Na/K pumps may coexist in the same cell suggests we need to carefully reevaluate previous studies. Moreover, our data illustrate the problem in maintaining a constant $[Na]_i$ over the course of an experiment. Though investigators have previously discussed this problem, there are usually no quantitative estimates of how much $[Na]_i$ changed and how greatly that change affected interpretation. As we have illustrated in some examples, changes in $[Na]_i$ of a few mM can lead to qualitatively incorrect conclusions, so one should question results that could be attributed to changes in $[Na]_i$. Despite these disclaimers, functionally different pumps and changes in $[Na]_i$ are simple physical factors, which, if taken into account, may explain many of the disparate results which appear in the literature, and thus simplify our view of Na/K pump function.

APPENDIX

Passive Electrical Properties

Table AI summarizes the passive electrical properties of the myocytes at $\psi_i = -60$ mV. The apparent area of myocyte membrane, assuming a smooth cylinder with the dimensions described in Table AI, is 86×10^{-6} cm^2. Assuming a specific membrane capacitance of 1 μF/cm^2, the total input capacitance of 189 pF translates to 189×10^{-6} cm^2 of actual membrane surface area, a value 2.2 times larger than the

TABLE A I

Passive Properties of Isolated Myocytes

	Cell length, L	Cell radius, a	t-System surface, S_t	Input capacitance, C_{in}	Input resistance	
					Normal R_{in}	$+Ba^{2+}$ R_{in}
Mean	127 μm	10 μm	0.57×10^{-4} cm^{-2}	189 pF	19 MΩ	197 MΩ
SD	± 30 μm	± 2 μm	± $.19 \times 10^{-4}$ cm^2	± 61pF	± 6 MΩ	± 61 MΩ
N	73	73	124	124	10	124

The value of S_t is estimated from C_{in} assuming 1 μF/cm^2 and the t-system capacitance, $C_t = 0.30\ C_{in}$ (see text).

apparent area. This difference arises in part because of the t-system of the myocyte and in part because the outer surface is not smooth. In Purkinje myocytes, which have no t-system, the area based on capacitance is 1.5 times larger than the apparent smooth value (Cohen et al., 1987). Page, McCallister, and Parver (1971) using stereological methods, report for rat ventricular myocytes the surface area of outer sarcolemma per unit volume of cell is 0.27 μm^{-1}, which translates to an outer surface area that is 1.35 times larger than the apparent smooth value. If guinea pig ventricular myocytes are similar in this regard, then the t-system contributes ~57 pF of the total capacitance or 30% of the total membrane area. This estimate corresponds well with structural data (B. Russel measured 32% in guinea pig, personal communication, and Page et al. [1971] reported 21% in rat), which were obtained by stereological analysis of electron micrographs.

The effect of the t-system on diffusion or current flow depends on its volume, V_t (cm^3), as well as surface area, S_t (cm^2). Moreover, current flow and diffusion are closely related phenomena that have exactly the same dependence on geometry. Based on the analysis by Mathias, Eisenberg, and Valdiosera (1977) the following diffusion equation describes the steady state changes, $[K]_t(r)$ (mol/cm^3), within the t-system lumen,

$$\frac{1}{r}\frac{d}{dr}\left(r\frac{d\Delta[K]_t(r)}{dr}\right) = -\frac{j_K}{V_t\zeta D_K},\ \Delta[K]_t(r_0) = 0. \tag{A1}$$

r_o is the fiber radius, ζ is a tortuosity factor, D_K (cm^2/s) is the diffusion coefficient and j_K (mol/s) is the total flux across all t-system membranes. The average perturbation in t-system K^+ is

$$\Delta[K]_t = \frac{2}{r_0^2}\int_0^{r_0}\Delta[K]_t(r)\,r\,dr. \tag{A2}$$

If the solution of Eq. A1 is averaged as in Eq. A2, the result is

$$\Delta[K]_t = -\frac{j_K}{l_t D_K}. \tag{A3}$$

The parameter l_t (centimeters) is a characteristic length that depends on the morphometry of the fiber and t-system. If the t-system volume and surface areas are uniform, as assumed in Eq. A1, then l_t can be morphometrically evaluated. Viz

$$l_t = V_t 8\zeta / r_0^2. \tag{A4}$$

However, if some regions of the t-system are not well connected with the bath or if there are local constrictions in t-system diameter, diffusional access would be reduced and l_t would be shorter than predicted by morphometric analysis. The virtu e of Eq. A3 is its generality, if one is not specific about l_t. An independent measure of l_t can be obtained electrically. Mathias, Eisenberg, and Valdiosera (1977) show the slowest electrical time constant reflecting restricted access to t-system membranes is given by

$$\tau_t = \frac{\rho}{l_t} C_t \tag{A5}$$

where $\rho = 60\ \Omega$-cm is bath solution resistivity and $C_t = 57$ pF is total t-system membrane capacitance. We performed frequency domain impedance studies of isolated myocytes, but no record had any detectable effects of the t-system, so we estimate that t_t is no slower than 16 μs (corresponding to ~10 KHz). Thus, $l_t = \rho\, C_t/\tau_t \geq 2.1$ μm from electrical measurements. Consider the morphometric definition of l_t in Eq. A4. For right circular cylinders of diameter d_t (cm), $V_t = S_t d_t/4$. In mammalian cardiac muscle, the smallest observed t-tubule diameter is $d_t = 0.03$ μm whereas more typical values are 0.3 μm (Sommer and Jennings, 1986). The tortuosity factor $\zeta \simeq 0.5$ (Mathias et al., 1977) so the smallest d_t gives $l_t \geq 1.7$ μm. Thus, the two methods produce a consistent lower limit for l_t of ~2 μm. With regard to changes in t-system K^+, the biggest transmembrane K^+ flux in our experiments is due to the pump. Hence, we estimate j_K assuming $2K^+$ are transported per cycle and assuming the t-system contributes 30% of the maximum $I_T = 182$ pA in Table II($[Na]_p = 80$ mM).

$$j_K \leq 0.5 \times 10^{-15}\ \text{mol/s} \tag{A6}$$

The worst case change in t-system K^+ is thus

$$\Delta[K]_t \leq 0.2\ \text{mM}, \tag{A7}$$

even this conservative upper limit is essentially negligible in our experiments.

We would like to thank Drs. Howard Haspel, Peter Brink, Jiamin Cui, and Jing Yi Shi for helpful comments throughout the development of this paper. Dr. Shelley Cohen did the statistical analysis of K^+-glycoside interaction and we are grateful. We would also like to thank Beverly Strozier for an excellent job preparing a difficult manuscript.

This work was suppported by the American Heart Association and National Institutes of Health grants HL 28958, HL 20558, HL 43731, and EY 06391.

Original version received 29 December 1993 and accepted version received 4 April 1995.

REFERENCES

Akera, T., Y.-C. Ng, R. Hadley, Y. Katano, and T. M. Brody. 1986. High affinity and low affinity ouabain binding sites in the rat heart. *European Journal of Pharmacology.* 132:137–146.

Apell, H. J., and W. Sturmer. 1992. Fluorescence study on cardiac glycoside binding to the Na,K-pump. *FEBS Letters.* 300:1–4.

Attwell, D., I. Cohen, and D. A. Eisner. 1981. The effects of heart rate on the action potential of guinea-pig and human ventricular muscle. *Journal of Physiology.* 313:439–461.

Berlin, J. R., A. J. Fielding, and N. Ishizuka. 1992. Identification of low and high affinity ouabain-sensitive Na pump current in voltage-clamped rat cardiac myocytes. *Annals of the New York Academy of Sciences.* 671:440–442.

Berrebi-Bertrand I., J. M. Maixent, F. G. Guede, A. Gerbi, D. Charlemagne, and L. G. Lelievre. 1991. Two functional Na^+/K^+-ATPase isoforms in the left ventricle of guinea pig heart. *European Journal of Biochemistry.* 196:129–133.

Breitwieser, G. E., A. A. Altamirano and J. M. Russel. 1987. Effects of pH changes on sodium pump fluxes in squid giant axon. *American Journal of Physiology.* 253:C547–C554.

Cohen, I. S., N.B. Datyner, G. A. Gintant, N. K. Mulrine, and P. Pennefather. 1987. Properties of an electrogenic sodium-potassium pump in isolated canine Purkinje myocytes. *Journal of Physiology.* 383:251–267.

Daut, J. 1983. Inhibition of the sodium pump in guinea-pig ventricular muscle by dihydro-ouabain: effects of external potassium and sodium. *Journal of Physiology.* 39:643–662.

Eisner, D. A., and T. W. Smith. 1991. The Na-K pump and its effectors in cardiac muscle. *In* The Heart and Caridovascular System. H. A. Fozzard, E. Haber, R. B. Jennings, A. M. Katz, and H. E. Morgan, editors. Scientific Foundations. Raven Press, NY. 863–901.

Gadsby, D. C., and M. Nakao. 1989. Steady state current-voltage relationship of the Na/K pump in guinea pig ventricular myocytes. *Journal of General Physiology.* 94:511–537.

Gao, J., R. T. Mathias, I. S. Cohen, and G. J. Baldo. 1992. Isoprenaline, Ca^{2+} and the Na^+-K^+ pump in guinea-pig ventricular myocytes. *Journal of Physiology.* 449:689–704.

Geering, K. 1990. Subunit assembly and functional maturation of Na,K-ATPase. *Journal of Membrane Biology.* 115:109–121.

Gick, G. G., M. A. Hatala, D. Chon, and F. Ismail-Beigi. 1993. Na,K-ATPase in several tissues of the rat: tissue-specific expression of subunit mRNAs and enzyme activity. *Journal of Membrane Biology.* 31: 229–236.

Glynn, I. 1988. The coupling of enzymatic steps to the translocation of sodium and potassium. *In* The Na^+, K^+ Pump. Part A. Molecular Aspects. Alan R. Liss, Inc., NY. 435–460.

Grupp, L, G. Grupp, and A. Schwartz. 1982. Digitalis receptor desensitization in rat ventricle: ouabain produces two inotropic effects. *Life Sciences.* 29:2789–2794.

Guillaume, D., T. Grisar, A. V. Delgado-Escueta, J. Laschet, and M. Bureau-Heeren. 1990. Two isoenzymes of Na^+, K^+-ATPase have different kinetics of K^+ dephosphorylation in normal cat and human brain cortex. *Journal of Neurochemistry.* 54:130–134.

Gupta, R. S., A. Chopra, and D. K. Stetsko. 1986. Cellular basis for the species differences in sensitivity to cardiac glycosides (digitalis). *Journal of Cellular Physiology.* 127:197–206.

Hagane, K., T. Akera, P. Stemmer, A.-Z. Yao, and C. Yokoyama. 1988. Comparison of [^{3}H] ouabain binding sites in intact cells and cell homogenates: apparent lack of glycoside receptors unrelated to sarcolemmal Na^+, K^+-ATPase in guinea-pig heart. *European Journal of Pharmacology.* 146:137–144.

Herzig, S., and K. Mohr. 1984. Action of ouabain on rat heart: comparison with its effect on guinea-pig heart. *British Journal of Pharmacology.* 82:135–142.

Inagaki, C., G. E. Lindenmayer, and A. Schwartz. 1974. Effects of sodium and potassium on binding of ouabain to the transport adenosine triphosphatase. *Journal of Biological Chemistry.* 249:5135–5140.

Isenberg, G., and V. Klockner. 1982. Calcium tolerant ventricular myocytes prepared by preincubation in a "KB-Medium." *Pflügers Archiv.* 395:16–18.

Jewell, E. A., and J. B. Lingrel. Comparison of the substrate dependence properties of the rat Na,

K- ATPase α1, α2, and α3 isoforms expressed in HeLa cells. 1991. *The Journal of Biological Chemistry.* 266:16925–16930.

Keynes, R. D. 1965. Some further observations on the sodium efflux in frog muscle. *Journal of Physiology.* 178:305–325.

Lauger, P. 1991. Electrogenic Ion Pumps. Sinauer Associates, Inc., Sunderland, MA.

Maixent, J. M., D. Charlemagne, B. de la Chapelle, and L. G. Lelievre. 1987. Two Na,K-ATPase isoenzymes in canine cardiac myocytes. *The Journal of Biological Chemistry.* 262:6842–6848.

Marty, A., and E. Neher. 1983. Tight-seal whole-cell recording. *In* Single-Channel Recording, Sakmann and Neher, editors. Plenum Publishing Corp., NY. 107–121.

Mathias, R. T., I. S. Cohen, and C. Oliva. 1990. Limitations of the whole cell patch clamp technique in the control of intracellular concentrations. *Biophysics Journal.* 58:759–770.

Mathias, R. T., R. S. Eisenberg, and R. Valdiosera. 1977. Electrical properties of frog skeletal muscle fibers interpreted with a mesh model of the tubular system. *Biophysics Journal.* 17:57–93.

Mogul, D. J., H. H. Rasmussen, D. H. Singer, and R. E. Ten Eick. 1989. Inhibition of Na-K pump current in guinea pig ventricular myocytes by dihydroouabain occurs at high- and low-affinity sites. *Circulation Research.* 64:1063–1069.

Nakao, M., and D. C. Gadsby. 1989. Na and K dependence of the Na/K pump current-voltage relationship in guinea pig ventricular myocytes. *Journal of General Physiology.* 94:539–565.

Orlowski, J., and J. B. Lingrel. 1988. Differential expression of the Na, K-ATPase α_2 subunit genes in a murine myogenic cell line. *Journal of Biological Chemistry.* 263:17817–17821.

Page E., L. P. McCallister, and B. Power. 1971. Stereological measurements of cardiac ultrastructures implicated in excitation-contraction coupling. *Proceedings of the National Academy of Sciences, USA.* 68: 1465–1466.

Rang, H. P., and J. M. Ritchie. 1986. On the electrogenic sodium pump in mammalian nonmyelinated nerve fibres and its activation by various external cations. *Journal of Physiology.* 196:183–221.

Russell, J. M., W. F. Boron, and M. S. Brodwick. 1983. Intracellular pH and Na fluxes in barnacle muscle with evidence for reversal of the ionic mechanism of intracellular pH regulation. *Journal of General Physiology.* 82:47–78.

Sachs, J. R. 1974. Interaction of external K, Na, and cardioactive steriods with the Na-K pump of the human red blood cell. *Journal of General Physiology.* 63:123–143.

Sachs, L. 1978. Applied Statistics. A Handbook of Techniques. Springer-Verlag. NY. 269 pp.

Sommer, J. R., and R. B. Jennings. 1986. Ultrastructure of cardiac muscle. *In* The Heart and Cardiovascular System. H. A. Fozzard, R. B. Jennings, E. Haber, A. M. Katz, and H. E. Morgan, editors. Raven Press, NY. 61–100.

Stimers, J. R., S. Liu, and T. A. Kinard. 1993. Effect of Na_i on activity and voltage dependence of the Na/K pump in adult rat cardiac myocytes. *Journal of Membrane Biology.* 135:39–47.

Stimers, J. R., S. Liu, and M. Lieberman. 1991. Apparent affinity of the Na/K pump for ouabain in cultured chick cardiac myocytes. *Journal of General Physiology.* 98:815–833.

Stimers, J. R., L. A. Lobaugh, L. Shi, N. Shigeto, and M. Lieberman. 1990. Intracellular sodium affects ouabain interaction with the Na/K pump in cultured chick cardiac myocytes. *Journal of General Physiology.* 95:77–95.

Sweadner, K. J. 1989. Isozymes of the Na^+/K^+-ATPase. *Biochimica et Biophysica Acta.* 988:185–220.

Sweadner, K. J., V. L. M. Herrera, S. Amato, A. Moellmann, D. K. Gibbons, and K. R. H. Repke. 1994. Immunological identification of Na, K-ATPase isoforms in myocardium. *Circulation Research.* 74: 669–678.

Wyman, J., and S. J. Gill. 1990. Binding and Linkage: Functional Chemistry of Biological Macromolecules. University Science Books. Mill Valley, CA.

Yu, H., F. Chang, and I. S. Cohen. 1993. Pacemaker current exists in ventricular myocytes. *Circulation*

Research. 72:232–236.

Zahler, R., M. Gilmore-Herbert, J. C. Baldwin, K. Franco, and E. J. Benz., Jr. 1993. Expression of α isoforms of the Na, K-ATPase in human heart. *Biochimica et Biophysica Acta.* 1149:189–194.

Zahler, R., M. Brines, M. Kashgarian, E. J. Benz, Jr., and M. Gilmore-Herbert. 1992. The cardiac conduction system in the rat expresses the novel α2 and α3 isoforms of the Na,K-ATPase. *Proceedings of the National Academy of Sciences, USA.* 89:99–103.